NCAR/TN-387+STR
NCAR TECHNICAL NOTE

August 1993

BIOSPHERE–ATMOSPHERE TRANSFER SCHEME (BATS) VERSION 1e AS COUPLED TO THE NCAR COMMUNITY CLIMATE MODEL

CLIMATE AND GLOBAL DYNAMICS DIVISION

NATIONAL CENTER FOR ATMOSPHERIC RESEARCH
BOULDER, COLORADO

NCAR TECHNICAL NOTES

The Technical Note series provides an outlet for a variety of NCAR manuscripts that contribute in specialized ways to the body of scientific knowledge but which are not suitable for journal, monograph, or book publication. Reports in this series are issued by the NCAR Scientific Divisions; copies may be obtained on request from the Publications Office of NCAR. Designation symbols for the series include:

EDD – Engineering, Design, or Development Reports

Equipment descriptions, test results, instrumentation, and operating and maintenance manuals.

IA – Instructional Aids

Instruction manuals, bibliographies, film supplements, and other research or instructional aids.

PPR – Program Progress Reports

Field program reports, interim and working reports, survey reports, and plans for experiments.

PROC – Proceedings

Documentation of symposia, colloquia, conferences, workshops, and lectures. (Distribution may be limited to attendees.)

STR – Scientific and Technical Reports

Data compilations, theoretical and numerical investigations, and experimental results

The National Center for Atmospheric Research is operated by the University Corporation for Atmospheric Research and is sponsored by the National Science Foundation. Any opinions, findings, conclusions, or recommendations expressed in this publication are those of the author(s) and do not necessarily reflect the views of the National Science Foundation.

Cover photograph by Carlye Calvin

CONTENTS

CONTENTS—Continued

Page

LIST OF TABLES

Page

LIST OF FIGURES

LIST OF APPENDICES

Page

PREFACE

A comprehensive model of land-surface processes has been under development suitable for use with various NCAR General Circulation Models (GCMs). Special emphasis has been given to describing properly the role of vegetation in modifying the surface moisture and energy budgets. The result of these efforts has been incorporated into a boundary package, referred to as the Biosphere-Atmosphere Transfer Scheme (BATS). The current frozen version, BATS1e is a piece of software about four thousand lines of code that runs as an offline version or coupled to the CCM. It includes (i) assignment of land type and soil information to each model grid square, (ii) calculation of soil, snow or sea-ice surface temperature in response to net surface heating and depending on soil or snow heat capacity and thermal conductivity, (iii) calculation of soil moisture, evaporation, and surface and groundwater runoff, (iv) specification of vegetation cover in terms of fractional ground shading and relative areas of transpiring and nontranspiring plant surfaces for different types of land-use, (v) surface albedo in terms of soil moisture, vegetation cover, and snow cover, including the shading of snow by vegetation, (vi) plant water budget including foliage and stem water storage, intercepted precipitation, and transpiration as limited by stomatal resistance and soil dryness, (vii) surface drag coefficients as a function of bulk Richardson number and vegetation cover, and (viii) determination of foliage temperature in response to energy-balance requirements and consequent fluxes of heat and moisture from the foliage to canopy air. Scientific studies have been pursued over the last decade to better establish the importance of various aspects of land-surface processes for climate and climate models and to gain confidence in the utility of application of BATS1e within a climate model. This report describes the physical processes, current numerical parameterizations, and some of the code structure of BATS1e.

Robert E. Dickinson
August 1993

ACKNOWLEDGMENTS

We thank K. Bluemel, A. Hahmann, X. Gao, F. Giorgi, A. Seth, J. Vaughn, and Y. Liu for contribution to the improvement of the code or Technical Note. We also thank Anji Seth for her careful review of the Technical Note. We thank Stephanie Shearer for formatting and editing the text and NCAR's Graphics Services and the Copy Center for their assistance in producing the color photograph on the cover of this report. R. E. Dickinson's permanent affiliation is the University of Arizona. A. Henderson-Sellers' permanent affiliation is Macquarie University, School of Earth Sciences, New South Wales, Australia. P. J. Kennedy is a member of the CGD Division at NCAR.

1. INTRODUCTION

The purposes of the biosphere–atmosphere transfer scheme (BATS), as coupled with the NCAR Community Climate Model (CCM), are to (a) determine the fraction of incident solar radiation that is absorbed by different surfaces and their net exchange of thermal infrared radiation, (b) calculate the transfers of momentum, sensible heat, and moisture between the earth's surface and atmospheric layers, (c) determine values for wind, moisture, and temperature in the atmosphere, within vegetation canopies, and at the level of surface observations, and (d) to determine (over land and sea ice) values of temperature and moisture quantities at the earth's surface. Included in the latter are the determination of the moisture content of soil, the excess rainfall that goes into runoff, and the physical state of the moisture at the surface, i.e., whether it is snow or water. To carry out these calculations, it is necessary to prescribe a predominant land–surface category for each surface grid point, and for those categories that have significant vegetative cover, to calculate the exchanges of moisture and energy among the vegetation and the soil and the air.

The earth's surface receives and emits various kinds of energy. The most important of these, from the viewpoint of physical processes, are (a) solar radiation, absorbed after undergoing atmospheric absorption and reflection, as determined by the radiative transfer subroutines and models of the surface albedo (depending on wavelength interval and solar zenith angle) (b) infrared radiation, emitted from the surface according to $\epsilon\sigma_s T^4$, where ϵ is the thermal emissivity, σ_s is the Stefan–Boltzmann constant, and T is the soil or vegetation temperature (downward atmospheric flux is obtained from the detailed radiative transfer calculation of the CCM or is parameterized); (c) sensible heat flux, by an aerodynamic transfer formula as proportional to the difference between some surface and overlying boundary–layer air temperatures; and (d) latent heat flux calculated similarly to (c) but proportional to specific humidity differences. The net energy received at the earth's surface melts snow, or warms the surface, or is conducted downward to be stored in lower layers.

Over a long–enough time period (a few days or more), the effect of heat storage within unfrozen soil becomes negligible. Over shorter times, it may be as important as the various energy fluxes. This "thermal inertia," depends on soil moisture, composition and overlying snow as well as on time scale.

One important feature of realistic climatic processes is the large diurnal variations of fluxes of sensible and latent heat over land surfaces. Indeed, even the sign of these quantities usually varies from day to night. These fluxes are strongly nonlinear functions of the static stability of the lowest atmospheric layers, and surface moisture is, in turn, a strongly nonlinear function of surface temperature, so that significant errors would be made in calculating these fluxes using diurnally averaged temperatures. Diurnal variations of temperatures at and near the ground are very significant properties of climate, as well as depending on other climatic properties such as soil moisture, intensity of incident solar flux, and convection in the boundary layer.

The presence of vegetation has a strong control over both diurnal and mean fluxes of energy and water. The physical characteristics of vegetation most important here are (a) absorption of solar radiation and consequent shading of the ground, (b) exchanges of sensible and latent heat with the atmosphere, and (c) the presence of canopy surface moisture. This moisture results from the film of water formed by dew or by intercepted rainfall; moisture beyond that which the foliage can hold drips to the ground. Over dry areas of the foliage, vapor pressure is controlled by stomatal openings (as parameterized by a stomatal resistance factor). Over forested areas, interception of rainfall by leaves and re-evaporation can remove most of the precipitation provided by a light drizzle. Furthermore, much of the transfer of moisture from the soil to the air is through leaf transpiration. Snowfall and frost are significantly affected by vegetative cover.

The present document revises the previous description (Dickinson *et al.,* 1981; Dickinson *al.*, 1986) and is intended to complement and explain the physics of the BATS code rather than serve as a substitute for it. Much additional documentation is provided internally in the FORTRAN code. Recent publications involving use of the BATS code include Dickinson (1991); Dickinson *et al.* (1989, 1991); Dickinson

and Kennedy (1991, 1992); Mearns *et al.* (1990); and Pitman *et al.* (1990). This report is divided as follows: Section 2 describes how land-cover and soils data were determined for the model and lists parameters dependent upon these classifications (these are data sets that are not required for the offline BATS1e model version, but are needed as input for coupling to a GCM). Section 2 also describes specification of land-surface albedo. (Section 3 summarizes what is involved in executing the code of that BATS surface physics package linked to the CCM). Section 3 describes how soil temperature is calculated. Section 4 gives the determination of soil moisture and snow cover for a nonvegetated grid square. Section 5 summarizes the calculation of momentum drag coefficients including the modifications needed for vegetation or for sea ice. Section 5 also describes how the model calculates sensible and latent fluxes over a nonvegetated surface. Section 6 describes what parameters are used to represent vegetation and how the model vegetation stores water. Section 7 summarizes the calculation of soil moisture and snow cover in the presence of vegetation. The appendices summarize some of the code notation.

Although the BATS treatment of surface processes is much more elaborate than those of conventional GCMs, its treatment of individual processes is still conceptually much simpler than the most elaborate models available for such, in particular for soil hydrology, plant water budgets, and snow physics.

a. Mathematical Symbols

For the convenience of the reader, we summarize here the mathematical symbols defined and used in the text.

α_f	Albedo of the vegetative canopy
α_{IR}	Snow albedo for near–infrared radiation
α_{IRD}	Snow albedo for diffuse near–infrared radiation
α_{IRO}	$=$ 0.65, albedo of new snow for near–infrared solar radiation with solar zenith angle less than 60°
α_V	Snow albedo for visible solar radiation
α_{VD}	Snow albedo for diffuse visible solar radiation
α_{VO}	$=$ 0.95, albedo of new snow for visible solar radiation with solar zenith angle less than 60°
$\Delta\alpha_g$	Increase of albedo due to dryness of soil surface
Δt	Model time step
ε	Thermal emissivity of ground
κ	R/C_p
λ	Wavelength of radiation
λ_s	Thermal conductivity
ρ_a	Density of surface air
ρ_i	Density of ice relative to water
ρ_s	Density of subsurface soil layer
ρ_{sw}	Density of snow relative to water
ρ_w	Volume of liquid water per unit volume of soil, weighted toward top layer as defined by Eq. (39)
ρ_{wsat}	Porosity or saturated soil water density
σ	Ratio of pressure p to surface air pressure p_s
σ_f	Fractional foliage cover for each grid point
σ_s	Stefan–Boltzmann constant
τ_{SNOW}	Nondimensional age of snow
τ_0	Time constant used in calculation of age of snow
ϕ	Soil water suction (negative potential)

ϕ_{MAX}	Soil water suction for permanent wilting of plants
ϕ_0	Soil water suction for saturated soil
Υ_{ro}	Maximum transpiration that can be sustained
Υ_w	Rate of transfer of water by diffusion to the upper soil layer from the lower; subscript zero denotes rate in the absence of gravity
a	Fraction of sea ice covered by leads
c_i	= Specific heat of ice $\simeq 0.45\ c_w$
c_s	Specific heat of subsurface layer
c_{sw}	= 0.49 c_w, specific heat of snow for unit snow density
c_w	= 4.186 $\times 10^6$ J m^{-3} K^{-1}, specific heat of water
$c_{A,F,V}$	Various bulk conductances as defined in the text
d_{ie}	Equivalent water depth of snow
d_{ice}	Depth of ice
d_s	= 10 S_{cv}/ρ_{sw} = 10 $\times$ snow depth
f	Ratio of soil evaporation to potential evaporation
f_d	Fraction of vegetation that is green and unwetted
f_w	Fraction of wet foliage
f_{SNOW}	Fraction of grid square covered by snow
$f(ZEN)$	Increase of snow albedo due to solar zenith exceeding 60°
g	Acceleration due to gravity
h_s	= $(S_g + (F^{\downarrow}_{IR} - F^{\uparrow}_{IR}) - F_s - L_{v,s}F_q - L_f S_m)$, heat balance at the surface
k	von Karman constant
k_s	Soil or snow thermal diffusivity
p_s	Surface air pressure
p_1	Lowest model level air pressure
q	Specific humidity
q_a	Lowest model level water–vapor specific humidity
q_{af}	Water–vapor specific humidity of the air within the foliage

q_g	Soil surface water–vapor specific humidity
$q_{g,s}$	Saturated specific humidity at soil surface temperature
q_s	Water–vapor specific humidity inside the leaves
r_a	Aerodynamic resistance factor $(1/(C_f U_{af}))$
r_s	Stomatal resistance factor
$r_{\ell a}$	Resistance to heat or moisture transfer through the laminar boundary layer at the foliage surface
r_F	$= r_{\ell a}/(\sigma_f L_{SAI})$, bulk foliage resistance
r_v	Average resistance for transfer of water vapor from foliage due to stomatal and aerodynamic resistance of the foliage surface
r_1	Rate of "snow aging" due to grain growth from vapor diffusion
r_2	Rate of "snow aging" due to melt water
r_3	Rate of "snow aging" from dirt and soot
r''	Fraction of potential evaporation from a leaf
s	Volume of water in soil divided by volume of water at saturation
s_i	Soil water as defined above in layer i
s_w	Soil water as defined above at permanent wilting point
s_0	S_{tw}/S_{twmax}
s_1	S_{rw}/S_{rwmax}
s_2	S_{sw}/S_{swmax}
t	Time
u_1	Lowest model level west–to–east wind component
u^*	Friction velocity (ρu^{*2} = surface momentum flux)
v_1	Lowest model level south–to–north wind component
z_0	Roughness length
z_1	Height of lowest model level
A_{LBG}	Albedo for bare soil
A_{LBL}	Albedo of plants for near infrared radiation

A_{LBS}	Albedo of plants for visible radiation
A_{LBGO}	Albedo for wet bare soil
B	Soil parameter defining change in soil water potential and hydraulic conductivity with soil water, a function of soil texture; also used as a symbol to represent forcing of surface soil
C_f	Coefficient of transfer between foliage and air in the foliage
C_p	Specific heat of air
C_s	Constant in snow albedo calculation (= 0.2)
C_D	Surface drag coefficient
$C_{D,F}$	Average momentum transfer coefficient over the grid square in the presence of vegetation
C_{DH}	Aerodynamic transfer coefficient for heat
C_{DN}	Drag coefficient for neutral stability
C_{DVEG}	Aerodynamic drag coefficient for the canopy
C_{DW}	Aerodynamic transfer coefficient for water vapor
C_N, C_S	Constants in snow albedo calculation (= 0.5, 0.2)
$C(ZEN)$	Cosine of the solar zenith angle
D	Average diffusivity for water flow through soil
D_f	Characteristic dimension of foliage elements in direction of wind flow
D_s	Rate of excess snow dropping from leaves per unit land area
D_w	Rate of excess water dripping from leaves per unit land area
D_{min}	Minimum value of soil diffusivity
D_{max}	$= B\phi K/\rho_{wm}$, maximum value of soil diffusivity
$E_{a,f,g}$	Water flux per unit land area; f refers to origin at foliage, g at ground, and a to the total flux; a superscript N, in Eq. (77)–(84), refers to the flux at the Nth iteration for leaf temperature
E_{tr}	Transpiration

E_{trmx}	Maximum transpiration the vegetation can sustain
F_c	Heat conduction through snow–covered sea ice or bare sea ice
F_s	Atmospheric sensible heat flux from ground to atmosphere
F_q	Moisture flux from ground to atmosphere
F_{qm}	Sustainable moisture flux through the soil surface, i.e., maximum as limited by diffusion
F_{sn}	Fraction of vegetation covered by snow
F_{vi}	Visible radiation incident at the top of the canopy
F_{AGE}	Snow age factor
$F_{IR}^{\downarrow}$ - $F_{IR}^{\uparrow}$	Net long–wave radiation flux from atmosphere to bare ground
$F_{SEAS}(T)$	Seasonal variation of vegetation cover with temperature (Eq. 1b)
G	Net water applied to the surface ($P_r + S_m - F_q$) in absence of vegetation
G_{HEAT}	Heat conduction rate from surface to underlying reservoir
$H_{a,f,g}$	Heat flux per unit land area to the atmosphere; f refers to origin at foliage, g at ground, a to total flux
K	Hydraulic conductivity of soil
K_0	Saturated soil hydraulic conductivity, equivalent to downward flow rate for saturated soil due to gravity
K_{VEG}	Land use/vegetation type in model
L_d	Unwetted fraction of leaf–stem area free to transpire
L_f	Latent heat of fusion
L_s	Latent heat of sublimation
L_v	Latent heat of evaporation
$L_{v,s}$	Either L_v or L_s, depending on whether T_g is greater than freezing or not
L_w	Ratio of wetted leaf stem area to total leaf stem area exchanging water with the atmosphere

L_{AI}	Leaf area index
L_{SAI}	Leaf–stem area index, sum of L_{AI} and S_{AI}
L_{SAIW}	Total vegetation surface that exchanges water with the atmosphere
M_f	Dependence of stomatal resistance on soil moisture
P	Precipitation rate
P_r	Rate of precipitation falling as rain
P_s	Rate of precipitation falling as snow
Q_c	Latent heat release
R	Gas constant
R_f	Dependence of the stomatal resistance on solar radiation
R_g	Leakage down to subsoil and groundwater reservoirs
Ri_B	Surface bulk Richardson number
R_m	Net radiation that would be absorbed by the vegetation if the foliage temperature = T_{g1}
R_n	Net radiation absorbed by the vegetation
R_s	Surface runoff
R_{ti}	Fraction of roots in the soil layer
R_w	Total runoff ($R_s + R_g$)
R_{OUGH}	Assigned roughness of vegetation types in model
$S^{\downarrow}$	Incident solar flux
S_f	Dependence of the stomatal resistance on temperature
S_g	Solar radiation absorbed over bare ground at earth's surface
S_m	Rate of snow melt
S_{cv}	Snow cover (liquid water equivalent)
S_{cv}/ρ_{sw}	Average snow depth
S_{gf}	Solar flux absorbed by vegetation
S_{rw}	Rooting zone soil water (maximum value of S_{rwmax})
S_{sw}	Surface soil water in upper layer of soil in meters (maximum value = S_{swmax})

S_{tw}	Total water in soil column of soil (maximum value = S_{twmax})
S_{AI}	Stem area index
T_{af}	Temperature within the foliage layer
T_c	Reference temperature for deciding whether precipitation is rain or snow
T_f	Temperature of foliage
Tg_1	Surface soil temperature
Tg_2	Subsurface temperature (depth of about 0.2 m)
Tg_3	Deep soil temperature (depth of about 2 m = annual average)
T_m	= 273.16 K, the melting or freezing temperature of pure water
T_B	Approximate freezing point of sea water
T_a	Air temperature of lowest model layer $\times(p_1/p_s)^{-\kappa}$
U_{af}	Magnitude of wind within the foliage layer
U_c	Subgrid–scale horizontal convection velocity
V_a	$= (u_1^2 + v_1^2 + U_c^2)^{1/2}$, strength of wind at the anemometer level
V_f	Dependence of stomatal resistance on vapor pressure deficit
W_{dew}	Total water stored by canopy per unit land area
W_{DMAX}	Maximum water the canopy can hold
W_{LT}	Soil dryness (or plant wilting) factor
W_{m1}	Rate of melting (freezing if negative) of surface soil water
W_{m2}	Rate of melting (freezing if negative) of subsurface soil water
Z_u	Depth of upper soil layer, fixed at 0.10 up to now
Z_r	Depth of soil rooting layer, varies typically from 0.5 to 2 m in thickness as a function of vegetation cover and/or land use
Z_t	Depth of total soil zone

2. DATA AND INTERFACE REQUIREMENTS FOR BATS COUPLED TO THE NCAR CCM

a. Overview and Coupling Requirements

To integrate BATS with the CCM or other atmospheric global or mesoscale model, a number of data fields must be supplied and other fields passed between BATS and the CCM/GCM at each model time step, as illustrated in Figure 1.

The atmospheric model defines from read in data sets a distribution of land points, including elevation, sea ice coverage, and ocean surface temperatures; the latter two can vary seasonally. A distribution of net energy fluxes over the ocean may also be prescribed as derived from a previous simulation and used for a flux corrected slab ocean temperature calculation. Data is read in for each land point, describing its assumed dominant vegetation cover, soil texture and soil color. Some vegetation and soil properties that vary interactively with BATS must be made available for calculation of albedo.

Interactive properties entering the albedo calculation include fraction of vegetation coverage, soil moisture, snow cover and snow age. The albedo routine must be tailored to match surface solar radiative fluxes provided by the atmospheric model. In particular, it must match the spectral intervals assumed by the model and treat separately direct solar beam and diffuse radiation.

Because the land versus ocean distributions of the prescribed data sets may not match those of CCM1, checks are made to provide soil and vegetation data to any CCM1 points that are classified land in the CCM but ocean in the land use data set. In CCM2, the prescribed data sets were edited to match the land versus ocean of the model. All the needed CCM fields are passed into a data structure adopted from an earlier NCAR GCM. The lowest model temperature is multiplied by σ^k for use as a "potential temperature." A routine named SOLBDC is called to obtain soil hydrological properties as a function of the soil-data fields. The routine BNDRY is then called to enter the main boundary package. Finally, the fields are transferred back into a form suitable for the CCM. Note, in particular, that we pass heat, moisture, and momentum fluxes evaluated for surface temperatures present at the finish of the boundary package for use in the vertical diffusion routine.

Subroutine BNDRY calls individual physical process subroutines and evaluates parameters common to several routines, as indicated in Figure 2. In particular, it provides the relative soil moisture from the model moisture and maximum soil moisture storage. It calls subroutine DRAG to obtain transfer coefficients between the lowest model layer and the surface (canopy plus ground). The coefficients depend on the lowest model altitude, surface roughness z_0–determined from surface cover–and a bulk Richardson number calculated from the strength of the lowest model-layer winds and the temperature difference between surface and lowest model layer.

Figure 1

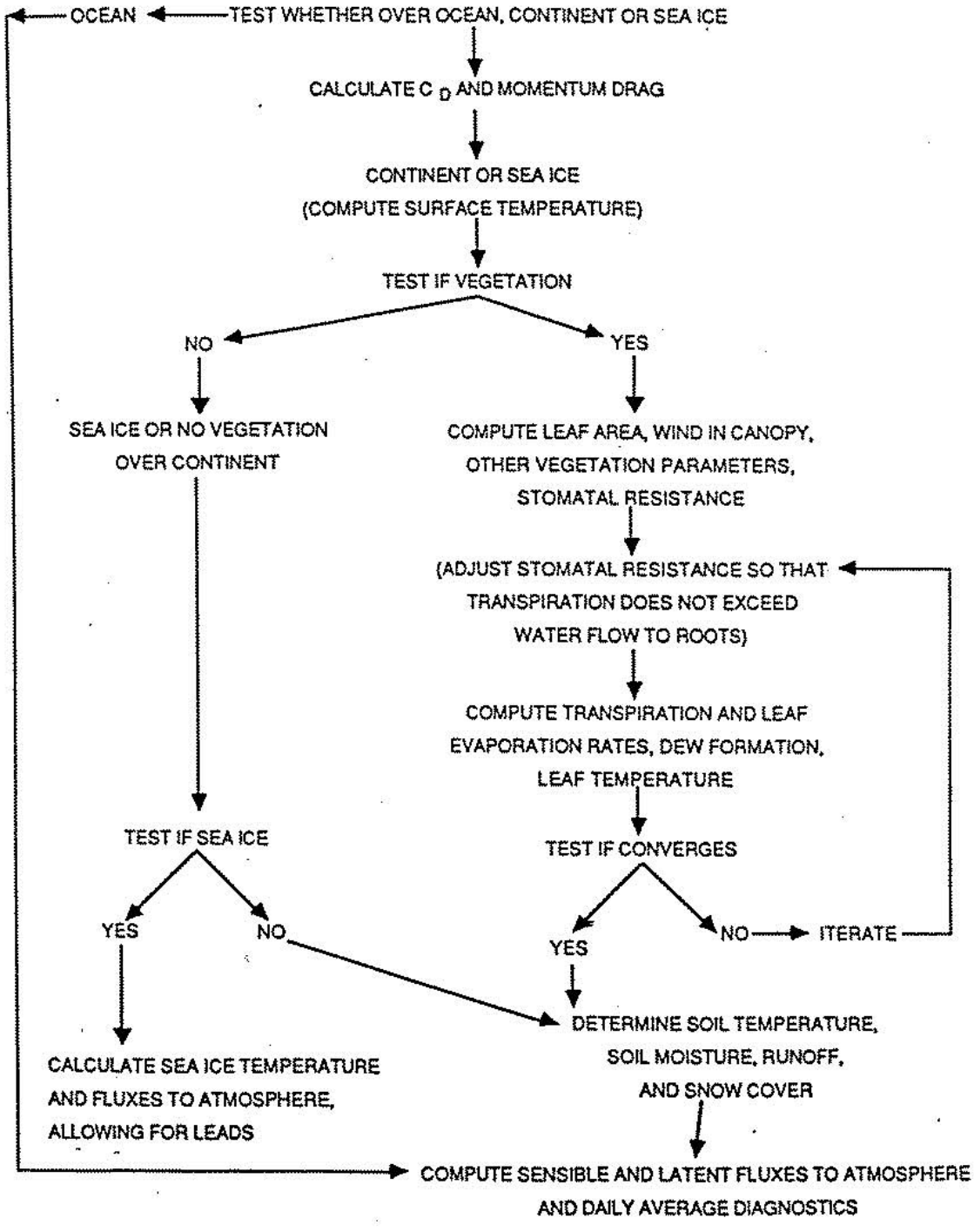
OCEAN
TEST WHETHER OVER OCEAN, CONTINENT OR SEA ICE
CALCULATE C D AND MOMENTUM DRAG
CONTINENT OR SEA ICE
(COMPUTE SURFACE TEMPERATURE)
TEST IF VEGETATION
NO
YES
SEA ICE OR NO VEGETATION
OVER CONTINENT
COMPUTE LEAF AREA, WIND IN CANOPY,
OTHER VEGETATION PARAMETERS,
STOMATAL RESISTANCE
(ADJUST STOMATAL RESISTANCE SO THAT
TRANSPIRATION DOES NOT EXCEED
WATER FLOW TO ROOTS)
COMPUTE TRANSPIRATION AND LEAF
EVAPORATION RATES, DEW FORMATION,
LEAF TEMPERATURE
TEST IF SEA ICE
TEST IF CONVERGES
YES
NO
YES
NO
ITERATE
DETERMINE SOIL TEMPERATURE,
SOIL MOISTURE, RUNOFF,
AND SNOW COVER
CALCULATE SEA ICE TEMPERATURE
AND FLUXES TO ATMOSPHERE,
ALLOWING FOR LEADS
COMPUTE SENSIBLE AND LATENT FLUXES TO ATMOSPHERE
AND DAILY AVERAGE DIAGNOSTICS

Figure 2

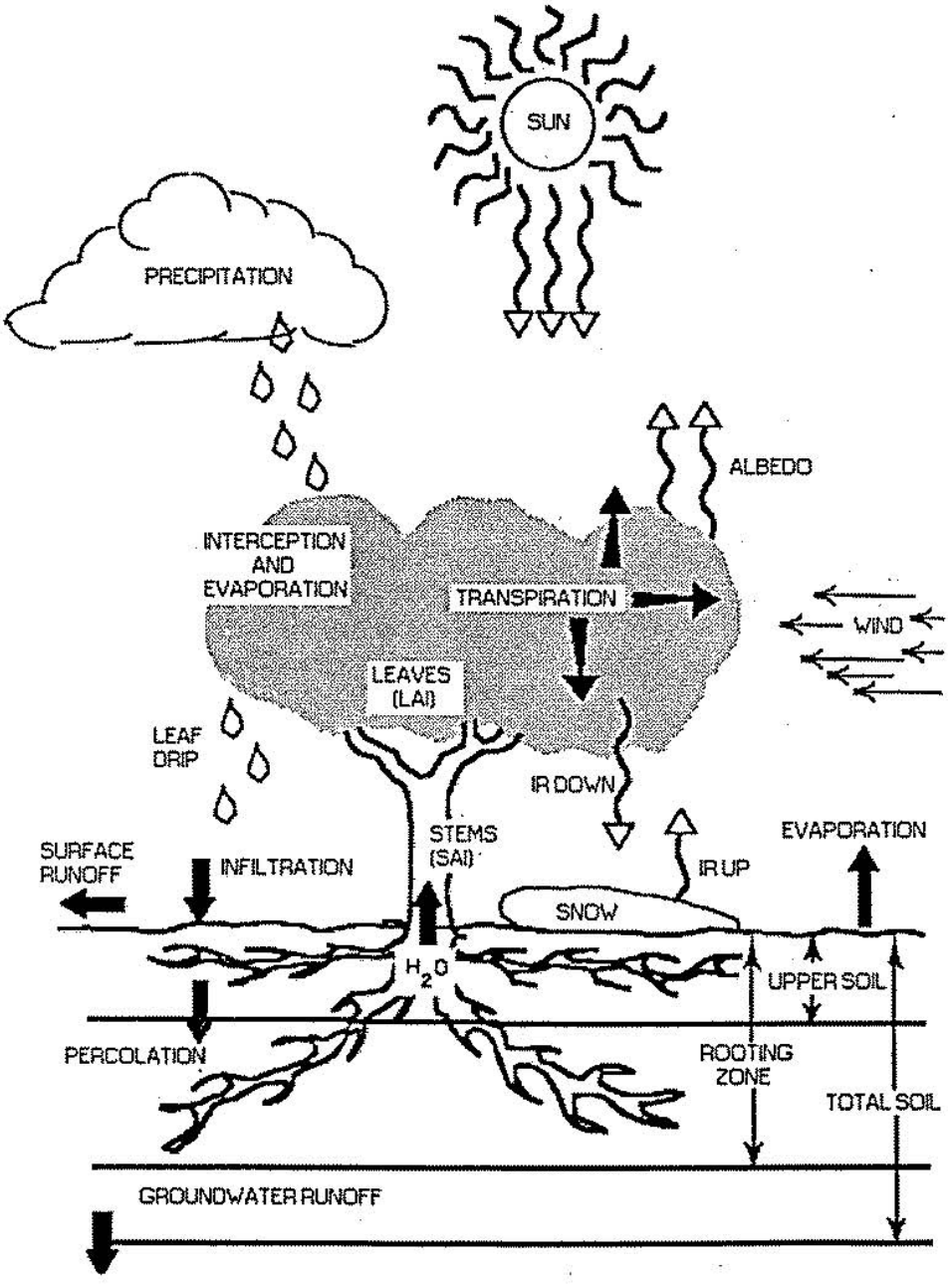
SUN
PRECIPITATION
ALBEDO
INTERCEPTION AND EVAPORATION
TRANSPIRATION
WIND
LEAVES (LAI)
LEAF DRIP
IR DOWN
STEMS (SAI)
EVAPORATION
SURFACE RUNOFF
INFILTRATION
IR UP
SNOW
H_2O
UPPER SOIL
PERCOLATION
ROOTING ZONE
TOTAL SOIL
GROUNDWATER RUNOFF

The vegetation part of the code is only executed for grid squares with vegetation cover greater than 0.001. A mean wind within the canopy is obtained from the mean wind outside the canopy times the square root of the drag coefficient, which equals the friction velocity u^*. The coefficient of transfer of heat and momentum from leaves is calculated. Foliage water is modified by intercepted rainfall. The temperature of the foliage (leaves) is calculated. Any rain or snow intercepted by leaves in excess of their maximum capacity is determined as falling to the ground and saved for soil-water or snow-budget calculations.

Returning to a calculation for all surfaces, we calculate rain or snow incident on the ground (minus any that was intercepted by the foliage) and partition soil evaporation into that from soil water and that from overlying snow. Routines are called to calculate the sea ice or the ground temperature and the budgets of snow cover and soil water. The updated temperatures, soil moisture, and foliage transpiration are used to determine net fluxes of heat and momentum from the surface to the lowest atmospheric model layer.

Surface-air properties are estimated for comparison with observations by using boundary-layer theory to interpolate between lowest model layer temperature and surface (ground, canopy-air or ocean). For connection to an overlying atmospheric model, temperature is evaluated at 10 m over ocean and 1.3 m over land, where it is assumed measured within a plot of short grass, embedded in the given cover type. The approximate formula used is

$$T_a = \widetilde{T}_{af} + \Delta T,$$

where

$$\widetilde{T}_{af} = T_{af}, \text{ if vegetated,}$$

$$\widetilde{T}_{af} = T_g, \text{ if nonvegetated,}$$

$$\Delta T = (T_1 - \widetilde{T}_{af}) z_{DELT},$$

$$z_{DELT} = \text{ minimum of}(1, b/[\log(z_1/z_0)]^2),$$

where $z_0 = 0.01$ m, and over land $b = 4.8(C_D/C_{DN})^{1/2}$ where C_D is the drag coefficient at z_1 and C_{DN} is its value for neutral conditions.

b. Land-Type Assignment

Currently, three global land-surface archives have been designed for incorporation into climate models–the vegetation data set of Olson *et al.* (1983), the vegetation and cultivation data of Matthews (1983, 1984) and the land use and soils data of Wilson (1984), described in Wilson and Henderson-Sellers (1985). The latter land-use data archives were used in the construction of a land-type data set for the CCM at R-15 resolution. The Olson *et al.* (1983) data has been used to construct a land use data set at T-42 resolution for use in CCM2. The implementation of the soils data of Wilson (1984) is described in the following subsection.

Matthews (1983, 1984) defines 31 classes of natural land type and prescribes the intensity of cultivation for each $1^o - \times - 1^o$ grid element. Wilson (1984) also uses base resolution of $1^o \times 1^o$ but defines two land-cover types for each land element–primary $\geq 50\%$ of the grid square, and secondary $< 50\%$ but $\geq 25\%$. She uses 53 land-cover classes including a number of cultivation categories. To simplify somewhat the CCM land-cover specification, both data archives were reduced to percentages of the 18 more basic land-cover classes shown in Table 1. Examples of the role of these different use classes are given in Figure 3.

Table 1. Vegetation/Land–Cover Types

1. Crop/mixed farming
2. Short grass
3. Evergreen needleleaf tree
4. Deciduous needleleaf tree
5. Deciduous broadleaf tree
6. Evergreen broadleaf tree
7. Tall grass
8. Desert
9. Tundra
10. Irrigated crop
11. Semi–desert
12. Ice cap/glacier
13. Bog or marsh
14. Inland water
15. Ocean
16. Evergreen shrub
17. Deciduous shrub
18. Mixed Woodland

Figure 3

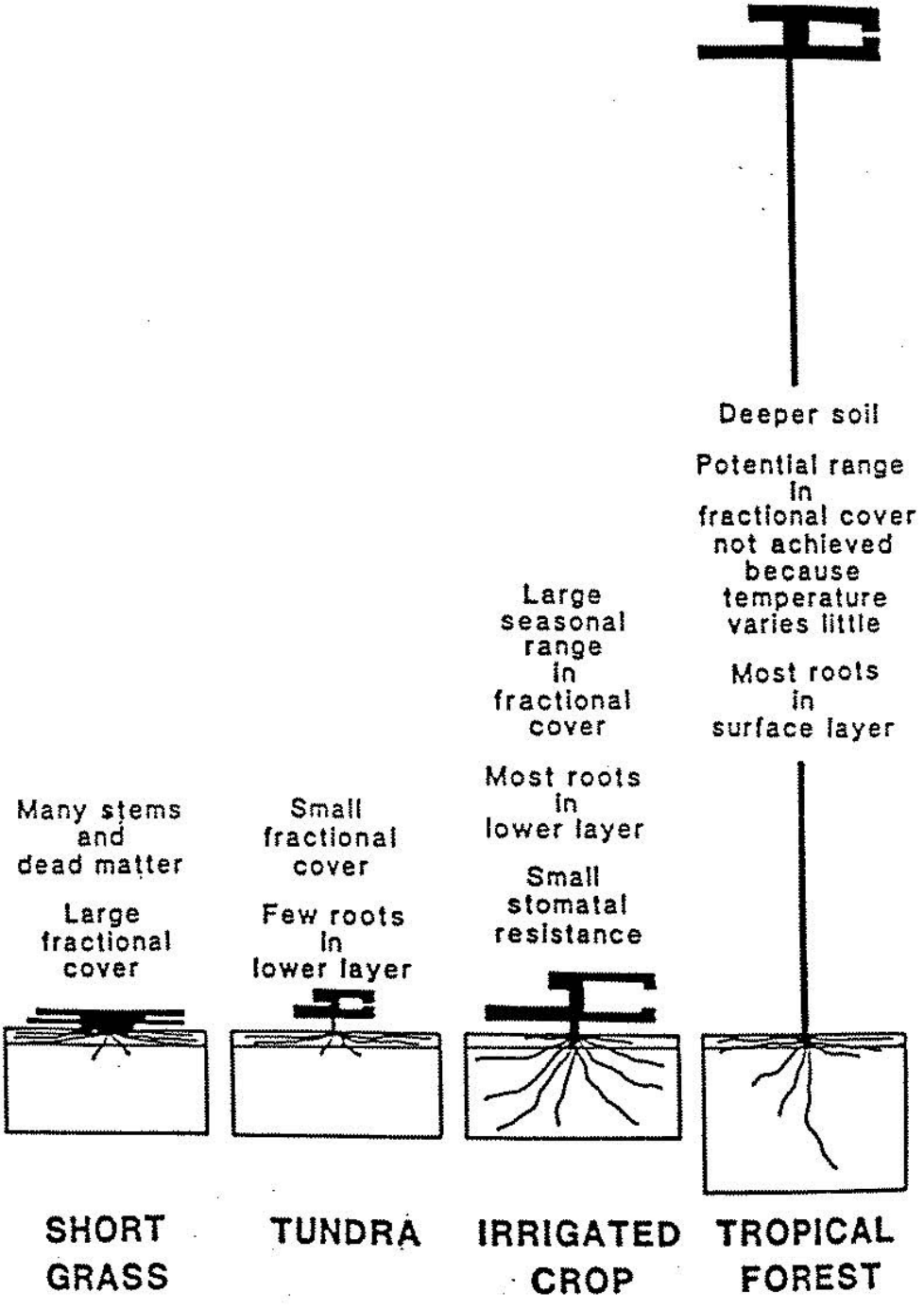
Deeper soil
Potential range in fractional cover not achieved because temperature varies little
Most roots in surface layer
Large seasonal range in fractional cover
Most roots in lower layer
Small stomatal resistance
Small fractional cover
Few roots in lower layer
Many stems and dead matter
Large fractional cover
SHORT GRASS
TUNDRA
IRRIGATED CROP
TROPICAL FOREST

Data sets at the R-15 resolution of approximately $4.5° \times 7.5°$ were derived from each of the 1°–sets and initially in terms of percentages of the 17 basic types in each grid element. Each grid element was assigned a dominant type except when use of type 18 (mixed woodland) seemed more appropriate. The dominant land types inferred from each data set were compared and if the classifications agreed, the result was incorporated into the final R-15 data set. At some model grid squares, differences occurred between the Matthews and the Wilson data sets, and two alternative or combined steps were taken. First, an average (of the two percentage components) was established and second, a comparison was made between this average and the ecotype classification of Olson *et al.* (1983), and subjective assessment was made as to what classification to use. The resultant archive is of 18 land–use classes defined on the model mesh. These 18 classes of land cover are used to define a wide variety of land surface, hydrological, and vegetation properties as described below.

The T-42 data set was derived by simply associating one of the 18 data types with each of the vegetation types of Olson *et al.* (1983), and the 0.5^o data was accumulated with model grid cells and the dominant type in each cell selected.

For each grid point, a value K_{VEG} is read into the model: $K_{VEG} = 0$ for all ocean grid points; $K_{VEG} = 1$ for all points with arable/mixed farming, etc. The assigned roughness length R_{OUGH} (given in Table 2) is used as the aerodynamic roughness, and the fraction of a grid square covered by snow f_{SNOW} is inferred according to the formula,

$$f_{SNOW} = f_{SN}/(1 + f_{SN}), \tag{1a}$$

with

$$f_{SN} = 0.1\ S_{cv}/(\rho_{sw} \times R_{OUGH}). \tag{1b}$$

The quantity $S_{cv}/(\rho_{sw})$ is the average snow depth and $R_{OUGH}/0.1$ is about half the average vertical extent of the surface objects. The quantity f_{SNOW}, calculated separately for the vegetated and nonvegetated parts of a grid square, determines what fraction of the area has the albedo of snow versus that of no snow. Over

vegetated areas, all vegetation covered by the snow pack is neglected by reducing the fraction of vegetation cover defined in subsection (b) by the factor $(1 - f_{SNOW})$.

For each land cover type, several vegetation parameters are required as indicated in Table 2. Besides roughness and albedo (discussed in next section) BATS requires a fractional vegetation σ_f and a leaf and stem area index LAI and SAI. The fractional vegetation and LAI range between minimum and maximum values according to a dependence on subsoil temperature

$$F_{SEAS}(T_{g2}) = 1 - 0.0016 \times (298.0 - T_{g2})^2 \qquad (1c)$$

when

$$273.16 < T_{g2} < 298$$

The fractional vegetation in the presence of snow is reduced by a factor $(1 - f_{SNOW})$ so that snow covered vegetation does not interact with the atmosphere. It is a current research topic to make these parameters more interactive with the model climate.

A number of the land–surface parameters defined as a function of land–cover type should, strictly, be made functions of soil type. However, for the present implementation, rooting ratios and upper and total soil depths (illustrated in Figure 1) remain a function of land–cover type only (Table 2). A number of parameters do vary with soil type and are described in the next subsection.

TABLE 2. VEGETATION/LAND COVER PARAMETERS

	Parameter	Land Cover/Vegetation Type*																	
		1	2	3	4	5	6	7	8	9	10	11	12	13	14	15	16	17	18
a)	Maximum fractional vegetation cover	0.85	0.80	0.80	0.80	0.80	0.90	0.80	0.0	0.60	0.80	0.10	0.0	0.80	0.0	0.0	0.80	0.80	0.80
b)	Difference between maximum fractional vegetation cover and cover at temperature of 269 K	0.6	0.1	0.1	0.3	0.3	0.5	0.3	0.0	0.2	0.6	0.1	0.0	0.4	0.0	0.0	0.2	0.3	0.2
c)	Roughness length (m)	0.06	0.02	1.0	1.0	0.8	2.0	0.1	0.05	0.04	0.06	0.1	0.01	0.03	0.0024	0.0024	0.1	0.1	0.8
d)	Depth of the rooting zone soil layer (m)**	1.0	1.0	1.5	1.5	2.0	1.5	1.0	1.0	1.0	1.0	1.0	1.0	1.0	1.0	1.0	1.0	1.0	2.0
e)	Depth of the upper soil layer (m)**	0.1	0.1	0.1	0.1	0.1	0.1	0.1	0.1	0.1	0.1	0.1	0.1	0.1	0.1	0.1	0.1	0.1	0.1
f)	Fraction of water extracted by upper layer roots (saturated)	0.3	0.8	0.67	0.67	0.5	0.8	0.8	0.9	0.9	0.3	0.8	0.5	0.5	0.5	0.5	0.5	0.5	0.5
g)	Vegetation albedo for wavelengths <0.7 μm	0.10	0.10	0.05	0.05	0.08	0.04	0.08	0.20	0.10	0.08	0.17	0.80	0.06	0.07	0.07	0.05	0.08	0.06
h)	Vegetation albedo for wavelengths >0.7 μm	0.30	0.30	0.23	0.23	0.28	0.20	0.30	0.40	0.30	0.28	0.34	0.60	0.18	0.20	0.20	0.23	0.28	0.24
i)	Minimum stomatal resistance (s m^{-1})	120	200	200	200	200	150	200	200	200	200	200	200	200	200	200	200	200	200
j)	Maximum LAI	6	2	6	6	6	6	6	0	6	6	6	0	6	0	0	6	6	6
k)	Minimum LAI	0.5	0.5	5.0	1.0	1.0	5.0	0.5	0.0	0.5	0.5	0.5	0.0	0.5	0.0	0.0	5.0	1.0	3.0
l)	Stem (& dead matter area index	0.5	4.0	2.0	2.0	2.0	2.0	2.0	0.5	0.5	2.0	2.0	2.0	2.0	2.0	2.0	2.0	2.0	2.0
m)	Inverse square root of leaf dimension ($m^{-1/2}$)	10	5	5	5	5	5	5	5	5	5	5	5	5	5	5	5	5	5
n)	Light sensitivity factor (m^2 W^{-1})	0.02	0.02	0.06	0.06	0.06	0.06	0.02	0.02	0.02	0.02	0.02	0.02	0.02	0.02	0.02	0.02	0.02	0.06

*See definitions in Table 1.

**Soil depths in code are in mm as are water storages to make the conversion factor 1.0 between water amounts and SI energy fluxes. All types have a total soil depth of 10 m to represent ground water storage.

c. Soil–Information Assignment

Wilson (1984) classifies soil color, texture, and drainage using the FAO Soil Map of the World (FAO/UNESCO, 1974) as the data source. Soil information is archived at 1°–×–1° resolution in three color classes, three texture classes, and three drainage classes. A soil–type archive has been constructed from these data on the R–15 and T-42 model grids. Eight color classes were derived with the scale stretched at the light end. Twelve texture classes, ranging from 1 = very coarse (equivalent to sand) to 12 = very fine (equivalent to heavy clay), were assigned by averaging the textures from the 1°–×–1° data set. Texture class 6 is comparable to a loam soil.

Soil properties have been associated with the twelve texture classes, dry and saturated albedos in two wavelength regions have been associated with the eight color classes.

d. Albedos

For each of the land grid points, three other variables are defined in subroutine ALBEDO–visible solar albedo of vegetation ($\lambda < 0.7\mu m$), near-infrared albedo of vegetation ($\lambda > 0.7\mu m$), and soil albedo. The values for the albedo of vegetation were determined from a variety of sources, in particular Monteith (1975, 1976), but also with reference to Monteith (1959), Kung *et al.* (1964), Barry and Chambers (1966), Federer (1968), Oguntoyinbo (1970), Stewart (1971), Tucker and Miller (1977), Rockwood and Cox (1978), Kriebel (1979), Fuller and Rouse (1979), and Kukla and Robinson (1980).

Gates *et al.* (1965) give spectral albedos of individual leaves. The near-infrared albedo for vegetation cannot be inferred from albedos of individual leaves since the high reflectivity (∼50%) and transmissivities of these surfaces imply that radiative transfer considerations are dominant (Dickinson, 1983). Our division into visible and near-infrared fluxes is largely based on the data of Tucker and Miller (1977), Kriebel (1979), and Fuller and Rouse (1979).

The albedo of the nonvegetated soil surface was determined from a variety of sources, e.g., Kondratyev (1969), Condit (1970), Idso *et al.* (1975), and Tucker and Miller (1977). The detailed distributions of the soil albedo depend upon soil type

and soil wetness. However, for vegetation cover σ_f of 0.80 or more, relatively little short-wave radiation reaches the ground so that these parameterizations become secondary.

The values for vegetation albedo presently used in subroutine ALBEDO are listed in Table 2. We have not been able to find much data on the albedos of branches and brown vegetation as contrasted to green (besides Federer, 1968, 1971), but we assume that it is the same as green. It appears that trunks and branches may have lower albedos by as much as 0.05, that red or brown leaves may have higher albedos by a much as 0.05, and that the spectral variation of albedo for either of these will differ from that of green leaves.

The albedo for bare soil A_{LBG} is taken to be

$$A_{LBG} = A_{LBGO} + \Delta\alpha_g(S_{sw}), \tag{2a}$$

where A_{LBGO} is the albedo for a saturated soil and where the increase of albedo due to dryness of surface soil is given for $\lambda < 0.7\mu$m as a function of the ratio of surface soil water content S_{sw} to the upper soil layer depth Z_u,

$$\Delta\alpha_g(S_{sw}) = 0.01(11 - 40S_{sw}/Z_u) > 0. \tag{2b}$$

This formulation is chosen so that soil albedos range in a nonlinear fashion between the saturated and dry values listed above. The term S_{sw} becomes small ($\leq$0.025 m) before the soil albedo shows a significant increase. Moisture is retained around the soil grains until $\sim$80% dryness occurs. The soil albedos for $\lambda > 0.7\mu$m are twice those for $\lambda < 0.7\mu$m. Dry and saturated soil albedos for the eight color classes used are shown in Table 3.

e. Snow Albedos

Snow albedos depend on spectral mix of the incident radiation/solar zenith angle, soot loading of the snow, snow depth, and grain size. Marshall (1989) has carefully developed a treatment of snow albedo with some advanced features not yet incorporated into BATS including combining the zenith dependence with grain size and depth dependence with soot loading.

BATS snow albedos still use the previous formulation inferred from the calculations of Wiscombe and Warren (1980) and the snow model and data of Anderson (1976):

$$\alpha_V = \alpha_{VD} + 0.4 f(ZEN)[1 - \alpha_{VD}], \tag{3}$$

$$\alpha_{IR} = \alpha_{IRD} + 0.4 f(ZEN)[1 - \alpha_{IRD}], \tag{4}$$

where α_V = albedo for $\lambda < 0.7\mu$ m, α_{IR} = albedo for $\lambda > 0.7\mu$ m, and the subscript D denotes diffuse albedos as given by

$$\alpha_{VD} = [1 - C_S F_{AGE}]\, \alpha_{VO}, \tag{5a}$$

$$\alpha_{IRD} = [1 - C_N F_{AGE}]\, \alpha_{IRO}, \tag{5b}$$

$$C_S = 0.2,\ C_N = 0.5,$$

and

α_{VO}	= 0.95, the albedo for visible radiation incident on new snow with solar zenith angle less than 60°
α_{IRO}	= 0.65, the albedo of new snow for near–infrared solar radiation with solar zenith angle less than 60°
$f(ZEN)$	= factor between 0.0 and 1.0 giving increase of snow visible albedo due to solar zenith angle exceeding 60°
$C(ZEN)$	= cosine of the solar zenith angle
F_{AGE}	= a transformed snow age defined below and used in this section to give the fractional reduction of snow albedo due to snow aging (assumed to represent increasing grain size and soot) for solar zenith angle less than 60°

The following parameterizations are used:

$$f(ZEN) = \frac{1}{b}\left[\frac{b+1}{1 + 2b\ C(ZEN)} - 1\right],\ f(ZEN) = 0 \text{ if } C(ZEN) > 0.5. \tag{6}$$

Equation (6) has the property for all b that it vanishes at $C(ZEN) = 0.5$ and is unity at $C(ZEN) = 0$ (sun on the horizon); b is adjustable to best available data—for now $b = 2.0$.

Snow albedo decreases with time due to growth of snow grain size and accumulation of dirt and soot. We parameterize the decrease term F_{AGE} in the above by

$$F_{AGE} = \tau_{SNOW}/[1 + \tau_{SNOW}]. \tag{7}$$

The nondimensional age of snow τ_{SNOW} is incremented as a model prognostic variable as follows:

$$\Delta\tau_{SNOW} = \tau_0^{-1}(r_1 + r_2 + r_3)\Delta t, \tag{8}$$

where $\tau_0^{-1} = 1 \times 10^{-6}$ s^{-1},

$$r_1 = \exp\left[5000\left(\frac{1}{273.16} - \frac{1}{T_{g1}}\right)\right],$$

$$r_2 = r_1^{10} \leq 1,$$

and

$$r_3 = 0.01 \quad \text{over Antarctica,} \quad = 0.3 \text{ elsewhere.}$$

The term r_1 represents the effect of grain growth due to vapor diffusion, the temperature dependence being essentially proportional to the vapor pressure of water.

The term r_2 represents the additional effect near and at freezing of melt water and r_3 the effect of dirt and soot.

A snowfall of 0.01 m liquid water is assumed to restore the surface age, hence albedo, to that of new snow. Since the precipitation in one model time step will generally be less than that required to so restore the surface when it snows for a

given time step, we reduce the snow age by a factor depending on the amount of the fresh snow in m, ΔP_s, as follows:

$$\tau_{SNOW}^{N+1} = (\tau_{SNOW}^{N} + \Delta\tau_{SNOW})(1 - 100\Delta P_s),\ \tau_{SNOW} > 0, \tag{9}$$

where $\Delta\tau_{SNOW}$ is defined as in Eq. (8).

TABLE 3. SOIL PARAMETERS

I/FUNCTIONS OF TEXTURE

	Parameter	Texture Class (from sand (1) to clay (12))											
		1	2	3	4	5	6	7	8	9	10	11	12
a)	Porosity (volume of voids to volume of soil)	0.33	0.36	0.39	0.42	0.45	0.48	0.51	0.54	0.57	0.60	0.63	0.66
b)	Minimum soil suction (mm)	30	30	30	200	200	200	200	200	200	200	200	200
c)	Saturated hydraulic conductivity (mm s^{-1})	0.2	0.08	0.032	0.013	8.9×10^{-3}	6.3×10^{-3}	4.5×10^{-3}	3.2×10^{-3}	2.2×10^{-3}	1.6×10^{-3}	1.1×10^{-3}	0.8×10^{-3}
d)	Ratio of saturated thermal conductivity to that of loam	1.7	1.5	1.3	1.2	1.1	1.0	0.95	0.90	0.85	0.80	0.75	0.70
e)	Exponent "B" defined in Clapp & Hornberger (1978)	3.5	4.0	4.5	5.0	5.5	6.0	6.8	7.6	8.4	9.2	10.0	10.8
f)	Moisture content relative to saturation at which transpiration ceases	0.088	0.119	0.151	0.266	0.300	0.332	0.378	0.419	0.455	0.487	0.516	0.542

II/FUNCTIONS OF COLOR

	Parameter	Color (from light (1) to dark (8)							
		1	2	3	4	5	6	7	8
a)	Dry soil albedo								
	< 0.7 μm	0.23	0.22	0.20	0.18	0.16	0.14	0.12	0.10
	≥ 0.7 μm	0.46	0.44	0.40	0.36	0.32	0.28	0.24	0.20
b)	Saturated Soil Albedo								
	< 0.7 μm	0.12	0.11	0.10	0.09	0.08	0.07	0.06	0.05
	≥ 0.7 μm	0.24	0.22	0.20	0.18	0.16	0.14	0.12	0.10

3. SOIL TEMPERATURE

The basis of the soil temperature model is described in Dickinson, (1988) which generalized the force restore method of Deardorff (1978). The following parameters are needed:

λ_s = thermal conductivity

$\nu_d = 2\pi/86400$ diurnal frequency

$\nu_a = \nu_d/365$ seasonal frequency

Δt = time step in s

$h_s = (S_g + F_{IR}^{\downarrow} - F_{IR}^{\uparrow} - F_s - L_{v,s}F_q - L_f S_m)$

the net soil surfaces heat impact, where

S_g = Solar flux absorbed over bare ground at earth's surface

$F_{IR}^{\downarrow} - F_{IR}^{\uparrow}$ = Net IR (long wave) flux from atmosphere to bare ground

F_s = Atmospheric sensible heat flux from ground to atmosphere

F_q = Atmospheric moisture flux from ground to atmosphere

$L_{v,s}$ = Latent heat of evaporation or sublimation

L_f = Latent heat of fusion

Q_{sf} = $L_f W_{m2} c_1/(\rho_s c_s d_1 c_2)$ = Rate of subsoil temperature change because of melting or freezing

S_m = Rate of snow melt

a. Surface Soil Temperature

Surface soil temperature T_{g1} is calculated from the following differential equation

$$C\Delta t \frac{\partial T_{g1}}{\partial t} + 2AT_{g1} = B \tag{10}$$

with the coefficients to be described below; B includes a term proportional to net surface heating.

$$B^{N+1} = B^N + B'(T_{g1}^{N+1} - T_{g1}^N) \tag{11a}$$

where T_{g1}^0 is the initial value of temperature from the previous time step (expression corrects latent and sensible fluxes to current temperature) and

$$A = 0.5\ \nu_d\ \Delta t \tag{11b}$$

$$B = B_{COEF}\ h_s + \nu_d\ \Delta t\ T_{g2} \tag{11c}$$

where h_s is the net surface heating, and

$$B_{COEF} = f_{SNOW}\ B_{COEFS} + (1 - f_{SNOW})\ B_{COEFB} \tag{11d}$$

where f_{SNOW} is defined by Eq. (1a). Also

$$B_{COEFS} = \frac{\nu_d\ \Delta t\ D_{ds}}{(\rho_s\ c_s)_s\ k_{sn}} \tag{11e}$$

$$B_{COEFB} = \frac{\nu_d\ \Delta t\ D_{db}}{(\rho_s\ c_s)_b\ k_{sb}} \tag{11f}$$

and the diurnal penetration depths are

$$D_{ds} = \left(\frac{2k_{sn}}{\nu_d}\right)^{1/2} \tag{11g}$$

$$D_{db} = \left(\frac{2k_{sb}}{\nu_d}\right)^{1/2} \tag{11h}$$

and where B' is the derivative of B with respect to temperature and is approximated by the temperature dependence of sensible and latent heat fluxes, defined later. In a more advanced approach where Tg is solved jointly with leaf temperatures (cf. Section 6g), an additional term is added to B correcting to T_f^{N+1}.

With Crank-Nicholson time differencing but using (11) to estimate B, we advance surface soil temperature from the Nth to $N + 1th$ time step (the change is limited to at most $\pm\ 10^o$), using

$$T_{g1}^{N+1} = \frac{B + (C - A - B')T_{g1}^N}{(C + A - B')} \tag{12}$$

k_{sn} = thermal diffusivity of snow, k_{sb} = thermal diffusivity of soil for diurnal wave, derived from soil water of upper soil layer.

And,

$$C = (1 + F_{CT1}) \tag{13}$$

where F_{CT1} is an additional thermal inertia of freezing to be described below (17b).

Snow diffusivity is based on: Corps. of Engineers (1956), Yen (1969), and Anderson (1976).

$$k_{sn} = k_{so}\ \rho_{sw}$$

where $k_{so} = (7.0 \times 10^{-7}/0.49)\ \mathrm{m^2 s^{-1}}$ and the heat capacity is

$$(\rho_s c_s) = \rho_{sw}\ c_{sw}$$

where

$$c_{sw} = 0.49 c_w$$

is the specific heat per unit snow density, and where ρ_{sw} is the density of snow relative to water.

Snow density is assumed given by

$$\rho_{sw} = 0.1 + 0.3 F_{AGE} \tag{14}$$

where F_{AGE} is the snow age factor.

Soil thermal diffusivity and heat capacity depend on soil moisture and texture (following deVries, 1963). For non frozen (bare) soil,

$$(\rho_s c_s)_b = (0.23 + \rho_w) c_w \tag{15}$$

$$k_{sb} = \frac{(2.9\rho_w + 0.04) k_c}{(1 - 0.6\rho_w)\rho_w + 0.09} \tag{16}$$

where

$$k_c = 10^{-7} \mathrm{m^2 s^{-1}} \times \mathrm{R_{AT}}$$

where R_{AT} is the ratio of the thermal diffusivity for a given texture to that for loam.

$$c_w = 4.186 \times 10^6 \text{J m}^{-3} \text{ K}^{-1}$$

is the specific heat of water and ρ_w is the volume of water per unit volume of soil. Separate ρ_w's are defined for the surface layer for the diurnal wave and for the root zone layer for the annual wave.

Modified thermal properties are used for frozen soil, i.e.

$$k_s = 1.4 \times 10^{-6} \text{ m}^2 \text{ s}^{-1}$$

and the contribution of water to $\rho_s c_s$ is reduced by 0.51 for that fraction of the water that is frozen. It is assumed that water freezes uniformly between 0^oC and -4^oC.

The term $F_{CT1} \geq 0$ parameterizes the contribution of the latent heat of freezing from the upper soil layer to surface energy balance, assuming this heating is given by the term

$$[\frac{D_u}{\sqrt{2} Z_u}] \frac{L_f (S_{sw} - F_{ru})}{\Delta T} \frac{\partial T_{g1}}{\partial t} \tag{17a}$$

where $\Delta T = 4^0$,
so that

$$F_{CT1} = \frac{\sqrt{2}\ L_f\ (S_{sw} - F_{ru})}{\rho_s\ c_s\ \Delta T\ Z_u} \geq 0 \tag{17b}$$

The term F_{ru} is the fraction of upper layer soil water that does not freeze. The term in square brackets in (17a), which is O(1), does not appear to be necessary and should be omitted in future implementations.

b. Snow Melt

In the presence of snow, snow melt is assessed from the energy required to balance h_s and change T_g, to 0^oC. If positive, inferred latent heat of melting is removed from h_s, limited by the remaining snow cover. This is written

$$S_m = \frac{[B + (C - A - B')T_{g1} - (C + A - B') \times 273.16]}{L_f \ B_{COEF}} \tag{18a}$$

$$0 < S_m \leq \ \Delta t \ S_{cv} \tag{18b}$$

The derivative of soil sensible and latent heat fluxes with respect to temperature use to evaluate B' are estimated in the absence of vegetation by

$$\frac{\partial F_s}{\partial T} \simeq \rho_a \ C_D \ C_p \ V_a \tag{19a}$$

$$\frac{\partial F_q}{\partial T} \simeq \rho_a \ C_D \ V_a \ f_g \ \frac{\partial q_s \ (T_{g1})}{\partial T} \tag{19b}$$

where f_g is a soil wetness factor determined from the soil evaporation formulation as the ratio of evaporation to that from a wet surface. In (19), we have neglected the contribution of the temperature dependence of C_D.

Estimates of flux derivatives with vegetation are described later. The flux derivative terms (19) are used to correct F_s and F_q to the $N+1$ time step to insure energy conservation.

c. Subsurface Temperature

The subsurface temperature T_{g2} is identified with the annual temperature wave in calculating from force-restore corresponding to temperature at a depth of roughly 1 m. As described in Dickinson, (1988),

$$(1 + F_{CT2})\Delta t \frac{\partial T_{g2}}{\partial t} + 2 \ A_2 \ T_{g2} = c_4 \ \nu_a \ \Delta t \ T_3 + \frac{D_a}{D_d} \ \nu_a \ \Delta t \tag{20}$$

where c_4 is a coupling coefficient to soil untouched by annual wave. At present $c_4 = 0$, except under permafrost where we take, $c_4 = 1.$, $T_3 = 271.0$. The term A_2 is

$$A_2 = (c_4 + \frac{D_a}{D_d})\ 0.5\nu_a\ \Delta t \tag{21}$$

in the absence of snow,

$$D_a = (\frac{\nu_d}{\nu_a})^{1/2}\ D_d \tag{21a}$$

and in the presence of snow, both D_a and D_d are weighted averages according to the depth of the snow,

$$D_d = W_{TDS}\ D_{ds} + (1 - W_{TDS})\ D_{db} \tag{21b}$$

$$D_a = W_{TAS}\ D_{as} + (1 - W_{TAS})\ D_{ab} \tag{21c}$$

with D_{as} and D_{ab} defined from D_{ds} and D_{db} with the factor of (21a). The weights for the snow contribution are

$$W_{TDS} = [1 - \exp\ (\frac{-2.\ S_{cv}}{\rho_{sw}\ D_{db}})] f_{SNOW} \tag{21d}$$

$$W_{TAS} = [1 - \exp\ (\frac{-2.\ S_{cv}}{\rho_{sw}\ D_{ab}})] f_{SNOW} \tag{21e}$$

where

$$F_{CT2} = \frac{\sqrt{2}\ L_f(S_{rw} - F_{rr})}{\rho_s\ c_s\ \Delta T\ Z_r} \geq 0 \tag{22}$$

with $F_{rr} = 0.15 Z_r$ the unfrozen soil water.

d. Over Bare Sea Ice or Snow–Covered Sea Ice

Over sea ice, the diurnal component of heat storage within the ice is neglected and replaced by steady conduction of heat from the underlying ocean. Hence, the sum of the components of energy fluxes becomes

$$h_s = S_g + F_{IR}^{\downarrow} - F_{IR}^{\uparrow} - F_s - L_v F_q - L_f S_m + F_c. \tag{23}$$

The heat conduction through snow–covered sea ice or bare sea ice, following Maykut and Untersteiner (1971) and Semtner (1976), is given by

$$F_c = \frac{K_{snow}(T_B - T_g)}{1 + R_{si}}$$

where

$$K_{snow} = 10^3 k_{sn} \rho_{sw}^2 c_{sw} / S_{cv},$$

where the factor of 10^3 is needed for S_{cv} to be in units of mm, and $k_{sn} c_{sw} = 7 \times 10^{-7} \rho_{sw}$, and

$$R_{si} = K_{snow}/K_{ice} = 1.4 \rho_{sw}^3 d_{ice} / S_{cv},$$

$$T_B = -2.0^\circ C.$$

The temperature at the surface of the ice and overlying snow changes according to

$$C_{EFF} \frac{\partial T_g}{\partial t} = h_s \tag{24}$$

where C_{EFF} is the effective heat capacity, assuming steady heat diffusion through the ice to determine the temperatures at the snow and ice midpoints and weighting the respective heat capacities with the ratios of these temperature tendencies to that of T_g, i.e.

$$C_{EFF} \;=\; 0.5 \; \{ \frac{1 + 2R_{si}}{1 + R_{si}} \; C_{SNOW} \;+\; \frac{R_{si}}{1 + R_{si}} \; C_{ICE} \} \tag{25}$$

where $C_{SNOW} = c_{sw} \; S_{cv}$, $C_{ICE} = c_i \; d_{ice}$, and where $c_i = 0.45 c_w$ and d_{ice} is the depth of ice, specified as a function of season, or computed.

4. SOIL MOISTURE AND SNOW COVER IN THE ABSENCE OF VEGETATION

For the soil moisture–snow cover specification, the earth's surface is divided into two regions—(1) oceanic regions (nonsea–ice–covered and sea–ice–covered regions), and (2) continental regions with and without snow cover. For the nonsea–ice–covered oceanic regions, the surface temperature T_{g1} is prescribed from observational data in the standard model. For other regions, the computation of T_{g1} depends on the current conditions of snow cover, soil moisture, type of surface, and temperature of the first layer of the atmosphere.

a. Precipitation (Rain and Snow)

The rainfall and latent heat release (Q_c) in each atmospheric layer depend in a complicated fashion on layer humidity and precipitation in overlying layers (the latter determining the phase of the precipitation).

The precipitation rate at the ground (P) is obtained as the sum of net precipitation from each layer. This precipitation is assumed to fall as snow P_s, if for the lowest model layer ($\sigma = 0.991$)$T_1 \leq T_c$, or as rain P_r if $T_1 > T_c$ (Auer, 1974), where $T_c = T_m + 2.2°$.

$$P_s = P,\ P_r = 0,\ \text{if } T_1 \leq T_c,$$

$$P_s = 0,\ P_r = P,\ \text{if } T_1 > T_c. \tag{26}$$

Corresponding latent heats should be used in the overlying GCM, if energy is to be conserved.

b. Soil Moisture Budget

Moisture incident on the ground either infiltrates the soil or is lost to surface runoff. For water, the soil is represented by 3-layers, all having a top surface at the soil-air interface, but with lower surface at increasing depth. We consider three parameters to represent soil moisture:

S_{sw} = Surface soil water representing water in the upper layer (depth Z_u) of soil

S_{swmax} = Maximum upper soil water

S_{rw} = Water in the rooting zone depth Z_r of soil

S_{rwmax} = Maximum root zone soil water

S_{tw} = Total water in the soil to depth Z_t

S_{twmax} = Maximum total water

In doing soil water budgets, S_{sw}, S_{rw}, and S_{tw} all gain the same amount of water from rainfall P_r, and lose the same amount from evaporation F_q and surface runoff R_s, since these fluxes occur at the soil surface.

Fluxes between soil layers affect the different (but overlapping) reservoirs differently. Their conservation equations are written (in absence of vegetation)

$$\frac{\partial S_{sw}}{\partial t} = G - R_s + \Upsilon_{w1} \tag{27a}$$

$$\frac{\partial S_{rw}}{\partial t} = G - R_s + \Upsilon_{w2} \tag{27b}$$

$$\frac{\partial S_{tw}}{\partial t} = G - R_s - R_g \tag{28}$$

where

$$G = P_r + S_m - F_q \tag{29}$$

G equals the net water applied to the surface, P_r = rainfall, S_m = snowmelt, and F_q = evaporation. Negative F_q represents dew formation. The terms F_q, R_s, R_g, and Υ_w are parameterized on the basis of a multilayer soil model (Dickinson, 1984). This parameterization is described in the remainder of this section.

c. Infiltration and Percolation to Ground Water

In principle, each grid square should have a distribution of soil types as established by its climate, vegetation, geology, etc. However, for now we assume a

single soil type for each grid square and with the following properties, mostly dependent upon the soil texture and listed in Table 3 (e.g., Campbell, 1974; Clapp and Hornberger, 1978). For the most part, the present parameterizations assume soil properties are constant with depth.

(a) Porosity = P_{ORSL} (see Table 3), i.e., at saturation 1 m^3 of soil holds P_{ORSL} (m^3) of water.

(b) Soil water suction (negative potential): $\phi = \phi_o s^{-B}$ where ϕ_o values are listed in Table 3; B ranges from 3.5 to 10.8 (Table 3), and s = volume of water divided by volume of water at saturation. For example, if $s = 0.3$ (the value at which transpiration is assumed to cease, as indicated in Table 3, line f), B = 5, and $\phi_o = 0.2$ mm, then $\phi = 82$ mm of tension. Note that $s = \rho_w / P_{ORSL}$.

(c) Hydraulic conductivity: $K_w = K_{wo} s^{2B+3}$, with values for K_{wo} (m s^{-1}) listed in Table 3 which represents the flow rate for saturated soil due to gravity.

Water represented by s diffuses through the soil with a diffusivity

$$D = -K_w \partial\phi/\partial s = K_{wo}\phi_o B s^{B+2}. \tag{30}$$

Besides the diffusive movement, there is gravitational drainage which dominates the flow for large–enough length scales. This provides the subsoil drainage expression,

$$R_g = K_{wo} s^{2B+3}, \tag{31}$$

e.g., at $s = 0.6$, B=5, and $K_{wo} = 8.9 \times 10^{-3}$ mm s^{-1}, $R_g = 1.3 \times 10^{-5}$mm s^{-1} (= 1.5 mm d^{-1}).

It is difficult to relate the drainage at the bottom of the subsoil layer (at 5 - 10 m) to soil properties at the surface; therefore, K_{wo} at that level has been assumed to be 4.0×10^{-4} mm s^{-1}, independent of soil type.

d. Evaporation

The evaporative terms F_q and the transfer between the upper soil layer and below are difficult to parameterize with sufficient generality. The current expressions are based on the behavior of a soil column that is initially at field capacity and

dried by a diurnally varying potential evaporation applied at the surface. Based on multilayer soil model integrations and theoretical arguments, we adopt the following parameterizations:

$$F_q = \text{minimum of } (F_{qp}, F_{qm}), \tag{32}$$

where F_{qp} = potential evaporation, and F_{qm} = maximum moisture flux through the wet surface that the soil can sustain. F_{qp} is calculated using Eq. (47) with $f_g = 1$ as the evaporation from a wet surface with the same aerodynamic characteristics as the soil surface, and

$$F_{qm} = E_{VMX0}\ \hat{B}\ s_2, \tag{33a}$$

where B is defined by

$$\hat{B} = s_1^{(3.+B_f)}\ s_2^{(B-B_f\ -1)}$$

$$E_{VMX0} = 1.02\ D_{max}\ C_k/(Z_u\ Z_r)^{1/2} \tag{33b}$$

using

$$D_{max} = B\phi_0 K_0/\rho_{wsat}, \tag{33c}$$

where ρ_{wsat} is the fraction of saturated soil filled by water, and K_0 in mm s^{-1} and ϕ_0 in mm the maximum conductivity and soil suction of Table 3, and defining

$$B_f = 5.8 - B\ [0.8 + 0.12(B-4)\ \log_{10}\ (100K_0)] \tag{33d}$$

and

$$C_k = (1 + 1550D_{min}/D_{max}) \times 9.76\ [\frac{B(B-6)+10.3}{B^2+40B}] \tag{33e}$$

Equation (33) was tested for values of ϕ_0 from 0.1 to 1.0 mm. The nominal value of D_{min} is 10^{-3} mm^2 s^{-1}, and the expression was tested for values of D_{min} from

10^{-2} mm^2 s^{-1} to 10^{-4} mm^2 s^{-1}. The general structure of the terms in (33a–e) is indicated from dimensional analysis and physical reasoning, but their detailed structure was inferred from trial–and–error numerical integrations. Since potential evaporation rarely exceeds 4×10^{-4} mm s^{-1}, soil much wetter than field capacity will generally evaporate at the potential rate.

Movement of water from the rooting zone into the surface soil layer is parameterized by

$$\Upsilon_{w1} = C_{f\ell 1}\ (s_1 - s_2) \tag{34}$$

and from the total column into the rooting zone by

$$\Upsilon_{w2} = C_{f\ell 2}\ (s_0 - s_1) \tag{35}$$

where the coefficients $C_{f\ell 1}$, $C_{f\ell 2}$ are given by

$$C_{f\ell 1} = E_{VMXR}\ (Z_u/Z_r)^{0.4}\ \times \hat{B} \tag{36}$$

where

$$E_{VMXR} = E_{VMX0}\ K_{0r}/K_0$$

$$C_{f\ell 2} = E_{VMXT}\ (Z_u/Z_r)^{0.5} \times s_0^{(2+B_f)} s_1^{(B-B_f)} \tag{37}$$

where Z_r is the depth of the soil active layer (between 500 and 2000 mm), Z_u is the depth of the surface soil layer (restricted to be between 10 and 200 mm thickness), where

$$E_{VMXT} = E_{VMX0} K_{01}/K_0$$

where K_{0r} is taken to be 0 or K_0 depending on whether the soil is frozen or not, and K_{01} to be 0 or K_0 depending on the presence of permafrost or not.

With the use of above expressions, water does not pond very frequently on the surface from saturation of the surface layer. It is thus necessary to assume

additional surface runoff near saturation, tuned to get the observed surface runoff (globally about half the total runoff), or to assume a subgrid–scale variation of rainfall intensity.

e. Surface Runoff

During periods of heavy rainfall or snowmelt and high soil moisture, much of the water incident on natural surfaces does not penetrate to ground–water reservoirs but, rather, flows immediately into streams and rivers.

The classical hydrology description is that such fast runoff flows on the surface in sheets or rivulets (overland flow). However, surface runoff is now described as occurring primarily over the fraction of a grid square where the soil has become saturated due to a high water table or to impermeable surface soil (the so–called variable source area). In some localities, near–surface flows, guided by underlying impermeable layers or subground air channels, are also important. Due to the complex nature of surface runoff processes, it is not possible to model them in detail. Thus, the surface runoff is usually inferred as a function of the rainfall history over a basin by analyzing the flood peaks in stream and river hydrographs. Although, in principle, there is no unique decomposition of a hydrograph into surface and ground–water runoff, in practice it is not difficult to devise such approximate divisions. L'vovich (1979), in particular, has provided annual average global maps of surface and ground–water runoff. He finds, on the average, that about half the total runoff is surface runoff. The physical basis for modeling hydrology on the small scale is reviewed in Kirby (1979). Available models for runoff simulation are summarized in Fleming (1975).

Guided by the criteria that there should be small surface runoff at the soil moisture of field capacity and complete surface runoff at saturated soil, we have parameterized surface runoff R_s by

$$R_s = (\rho_w/\rho_{wsat})^4 G, \quad T_{g1} \geq 0°C,$$

$$= (\rho_w/\rho_{wsat})G, \quad T_{g1} < 0°C, \tag{38}$$

where ρ_{wsat} is the saturated soil water density and ρ_w is the soil water density weighted toward the top layer, as defined by

$$\rho_w = \rho_{wsat}\frac{(s_1 + s_2)}{2}, \tag{39}$$

and G is defined by (29). For negative $G, R_s = 0$. If the subsurface temperature is below freezing, the fraction of surface runoff is increased. This allows crudely for the effect of frozen ground.

f. Snow Cover

The most detailed model of snow energy balance and melt processes to date has been given by Anderson (1976). He models, in particular, water and energy transfer and density changes throughout the snow column. By contrast, we model explicitly only the snow–surface processes. There is no explicit distinction between subsurface snow versus soil temperature, i.e., T_{g2} refers, in principle, to a subsurface snow temperature after more than a few centimeters of liquid equivalent snow have accumulated. The most serious conceptual errors occur during time of snow melt or rainfall on a snowpack. We put water on the snow surface directly into the soil, whereas real melt or rain water has to percolate through the snow pack and may refreeze. We also implicitly neglect melting at the bottom of the snow pack due to heat conducted from the ground (ground melt) unless this heat reaches the top snow surface.

If it is snowing or if there is snow cover, we first check to see if T_g is 0.0°C, and if so, compute the snow melt rate before computing the surface temperature. (cf. Section 3).

If S_m calculated from Eq. (18a) exceeds the snow cover, S_m is set to the snow cover and the ground temperature is calculated from Eq. (10), including the heat loss required to melt the snow. If snow remains after melting the snow amount

given by Eq. (18), we set

$$T_g = 0^\circ \text{ C}.$$

The snow cover is updated from

$$\frac{\partial S_{cv}}{\partial t} = P_s - F_q - S_m\,, \tag{40}$$

where S_{cv} is the snow–cover amount measured in terms of liquid water content, P_s is the snow precipitation rate, and F_q equals the rate of sublimation.

5. DRAG COEFFICIENTS AND FLUXES OVER BARE SOIL

Drag coefficients over land are quite variable (e.g., cf. Garratt, 1977). Thus, in the BATS scheme, C_D is calculated as a function of C_{DN}, the drag coefficient for neutral stability, and Ri_B is the surface bulk Richardson number, i.e.,

$$C_D = f(C_{DN}, Ri_B), \tag{41}$$

where C_{DN} is the drag coefficient for neutral stability, Ri_B is the surface bulk Richardson number,

$$Ri_B = \frac{gz_1(1 - T_{g1}/T_a)}{V_a^2}, \tag{42}$$

where $V_a^2 = u_1^2 + v_1^2 + U_c^2$ with T_{g1} the surface soil (or snow or ice) temperature and T_a, u_1, v_1 the air temperature $\times\ (p_s/p_1)^\kappa$ and wind components at z_1, where z_1 is the height of the lowest model level, g = acceleration due to gravity, and

$$\begin{aligned} U_c &= 0.1 \text{ m s}^{-1}, \quad \text{if } T_{g1}/T_a < 1, \\ &= 1.0 \text{ m s}^{-1}, \quad \text{if } T_{g1}/T_a > 1 \end{aligned} \tag{43}$$

Also, modifying slightly the formulae given in some notes of Deardorff (personal communication), we take for $Ri_B < 0$

$$C_D = C_{DN}(1 + 24.5(-C_{DN}Ri_B)^{1/2}), \tag{44a}$$

and for $Ri_B > 0$

$$C_D = C_{DN}/(1 + 11.5Ri_B). \tag{44b}$$

For use in CCM2, this formulation for stability dependence is replaced with that of CCM2. The neutral drag coefficient is obtained from mixed–layer theory as

$$C_{DN} = \left[\frac{k}{\ln(z_1/z_0)}\right]^2, \tag{45}$$

where $k = 0.40$, the von Karman constant, and z_0 is the roughness length. For water surfaces, we take $z_0 = 2.3 \times 10^{-4}$ m so that $C_{DNW} = 0.0014$. For bare land, we take $z_0 = 10^{-2}$ m so that $C_{DNL} = 2.4\ C_{DNW}$.

The sensible and latent heat fluxes over water, sea ice, or bare surfaces are obtained using the above defined momentum drag coefficients as follows:

$$F_s = \rho_a C_p C_D V_a (T_{g1} - T_a), \tag{46}$$

where ρ_a is the surface air density, C_D the aerodynamic drag coefficient for heat, C_p the specific heat for air, and V_a the wind speed. Similarly, the moisture flux (from the surface) to the atmosphere F_q is given by

$$F_q = \rho_a C_D V_a f_g (q_g - q_a), \tag{47}$$

where q_g is the saturated specific humidity at the temperature of the surface (ground, snow, ice, or water), q_a is the specific humidity of the model lowest level, and f_g is a wetness factor, which has the value of 1.0 except for diffusion–limited soil surfaces, where it is defined by the ratio of actual to potential ground evaporation, i.e.,

$$f_g = F_q / F_{qp}.$$

For the leaf temperature calculation, drag coefficients are determined as above except that a lower limit is imposed of the minimum of $C_{DN}/4$ or 6×10^{-4} and drag coefficient derivatives with respect to temperature are obtained from Eqs. (42), (44a), (44b), except that the derivative of (44a) is replaced by the derivative of (44b) at $Ri_B = 0$, for small values of Ri_B, where it exceeds that value.

Over vegetated grid squares, the neutral drag coefficient is estimated by a linear combination for drag coefficients for vegetation, for bare soil, or over snow. We assume that the snow coefficient has the value C_{DNS}. If $C_{D,FN}$ denotes the neutral drag coefficient over the grid square, and σ_f the more connected vegetation fraction, then

$$C_{D,FN} = \sigma_f \, C_{FN}(1-F_{sn})+(1-\sigma_f)(1-S_{cv})C_{DNL} \, +\{\sigma_f \, F_{sn}+(1-\sigma_f) \, S_{cv}\} \, C_{DNS} \tag{48}$$

where C_{FN} is the local drag coefficient over vegetation, determined using Equation (44) and $z_0 = z_{0v}$ tabulated for the given vegetation type, and S_{cv} is the fraction of ground covered by snow, F_{sn} is the fraction of vegetation covered by snow, and C_{DNL} is the drag coefficient for bare land. Over tall vegetation, a "displacement" height is subtracted from z, in Eq. (44).

BATS uses

$$S_{cv} = \text{snowdepth}/(0.1m + \text{snowdepth})$$

$$F_{sn} = \text{snowdepth}/(10 z_{0v} + \text{snowdepth})$$

For energy flux calculations in the next section, we ignore snow covered vegetation, i.e.

$$\sigma_f = (1 - F_{sn})\sigma_f^0$$

where σ_f^0 is σ_f in the absence of vegetation.

6. ENERGY FLUXES WITH VEGETATION

Our treatment of vegetation within the CCM is not dissimilar to the usual one–layer formulation in the micrometeorological literature ascribed to Monteith (e.g., Thom and Oliver, 1977), except that we consider separate ground–energy equations and separate resistances for transfer from above the canopy to air within the canopy and from air within the canopy to the foliage surfaces and allow for partial wetting of the canopy. In applying a self–consistent model rather than observations as is usually done, it is necessary to derive variables within the canopy in terms of lowest atmospheric model–layer variables. At each land grid point, we prescribe a fractional vegetation cover σ_f as described in section 2 (Deardorff, 1978; Shuttleworth, 1978).

a. Parameterization of Foliage Variables

The one–sided surface area of vegetation per unit area of ground consists of transpiring surfaces specified by a leaf area index, i.e., (L_{AI}) and nontranspiring surfaces (including dead vegetation) specified by a stem area index (S_{AI}). The S_{AI} is a constant for each land type, whereas the L_{AI} has a seasonal variation, using the same dependence on subsoil temperature as used for σ_f,

$$L_{AI} = L_{AI}^{MIN} + F_{SEAS}(T_{g2}) \times (L_{AI}^{MAX} - L_{AI}^{MIN}), \tag{49}$$

where the seasonal factor $F_{SEAS}(T)$ is defined by Eq. (1c). We denote the sum of L_{AI} and S_{AI} the L_{SAI} (leaf stem area index), i.e., $L_{SAI} = L_{AI} + S_{AI}$. To include evaporation from wetted stems and leaves, we follow Deardorff in defining the fractional area of the leaves covered by water as

$$\widetilde{L}_W = \left(\frac{W_{dew}}{W_{DMAX}} \right)^{2/3}, \tag{50a}$$

where W_{dew} is the total water intercepted by the canopy and W_{DMAX} is the maximum water the canopy can hold, as defined in the next subsection. The same expression is used for the stems. The fraction L_d of foliage surface free to transpire is then defined by

$$L_d = (1.0 - \widetilde{L}_w) L_{AI} / L_{SAI}. \tag{50b}$$

The values presently used for defining L_{AI} and S_{AI} are listed in the land–cover type parameter list for Table 2. The grassland values were obtained from Ripley and Redman (1976). Other values are based on a wide variety of inputs. The $S_{AI} = 0.5$ of class 1 (cropland) corresponds to the 0.1 used by Deardorff (1978) for S_{AI}/L_{AI}.

Also needed is the magnitude of wind within the foliage layer taken to be

$$U_{af} = V_a C_D^{1/2}. \tag{51}$$

b. Vegetation Storage of Intercepted Precipitation and Dew

When it rains, the surfaces of vegetation become covered with a film of water before drip through and stem flow carry water to the ground. This water can then reevaporate to the air, but at the same time transpiration is suppressed over wet green leaves. Similarly, the formation of nighttime dew can keep foliage cool in the morning and suppress transpiration. Typical values for reevaporation of intercepted rainfall are in the range of 10 to 50% of rainfall, depending primarily on rainfall intensity. The suppression of transpiration by wet leaves has been less studied but is probably also significant. Snowfall is also intercepted by foliage, and frost formation on foliage commonly occurs. These are of somewhat less significance for the water budget because of lower evapotranspiration rates at low temperatures. Hence, it is reasonable to assume that vegetation storage of solid water is the same as liquid water. In doing so, we ignore the larger initial water storage of snow interception and its frequently more rapid removal by blowoff. We assume a maximum water storage of 0.0001 m $\times$ L_{SAI}. The water stored per unit land–surface area is calculated from the incident precipitation and difference between transpiration and water flux to the plant surface, i.e.,

$$\frac{\partial W_{dew}}{\partial t} = \sigma_f P - E_f + E_{tr}. \tag{52}$$

If $W_{dew} > W_{DMAX} = 0.0001$ m $\times \sigma_f L_{SAI}$, then W_{dew} is set equal to W_{DMAX} and the excess leaf moisture is added to the precipitation on the soil, either as water or

snow, depending on whether or not the snowfall criteria are satisfied. More general drip formulae are discussed by Massman (1980).

c. Foliage Fluxes

We first discuss the evaporation from wet foliage. The water flux from dry foliage follows similar considerations but, in addition, the resistance to water flux by stomata needs consideration. The water on wet foliage (leaves and stems) evaporates per unit wetted area according to

$$E_f^{WET} = \rho_a r_{\ell a}^{-1}(q_f^{SAT} - q_{af}), \tag{53}$$

where q_f^{SAT} is the saturation water–vapor specific humidity at temperature of the foliage T_f, q_{af} is the water–vapor specific humidity ratio of air within the canopy, and $r_{\ell a}$ is the aerodynamic resistance to moisture and heat flux of the foliage molecular boundary layer per unit foliage projected area. Multiplication of Eq. (53) by L_{SAI} gives the total flux from wetted surfaces. Equation (53), if negative, gives the rate of accumulation of dew on foliage whether wet or not.

The conductance for heat and vapor flux from leaves is given by

$$r_{\ell a}^{-1} = C_f \times (U_{af}/D_f)^{1/2}, \tag{54}$$

where $C_f = 0.01$ m s$^{-1/2}$, D_f is the characteristic dimension of the leaves in the direction of wind flow, and U_{af} is the magnitude of the wind velocity incident on the leaves. Equation (54) corresponds to models of laminar boundary layers past flat plates (as discussed in Gates, 1980). Equation (53) gives the evaporation at each surface within the canopy; however, a different definition of Eq. (54) would be needed to apply it to stems and needles. It is also assumed that Eq. (53) can be applied to the canopy as a whole.

Similar to (53), the heat flux from the foliage is given by

$$H_f = \sigma_f L_{SAI} r_{\ell a}^{-1} \rho_a C_p (T_f - T_{af}). \tag{55}$$

The flux E_f canopy surfaces that are only partly wet, with wetted fraction denoted $\tilde{L}_w$; now follows from Eq. (53) as

$$E_f = r'' E_f^{WET}, \tag{56}$$

where

$$r'' = 1 - \delta(E_f^{WET}) \left[1.0 - \tilde{L}_w - L_d \left(\frac{r_{\ell a}}{r_{\ell a} + r_s} \right) \right], \tag{57}$$

where r_s = 'stomatal' resistance to be discussed further, $\tilde{L}_w$ is defined by Eq. (49), L_d is defined by Eq. (50) and where δ is a step function and is one for positive argument and zero for zero or negative argument. The fraction of wetted area over nontranspiring foliage is assumed to be the same as that for transpiring foliage.

Transpiration E_{tr} occurs only from dry leaf surfaces and is only outward,

$$E_{tr} = \delta(E_f^{WET}) L_d \left(\frac{r_{\ell a}}{r_{\ell a} + r_s} \right) E_f^{WET}. \tag{58}$$

The above formulation neglects the likely small temperature differences between wet and dry surfaces, as well as the effects of several other possible inhomogeneities. For example, many plants, such as hardwood trees, have leaf stomata that occur only on the underside of leaves, whereas leaf water may be stored largely on the upper surface of the leaves.

d. Stomatal Resistance

The term stomatal resistance, as used here, refers to the total mechanical resistance encountered by diffusion from inside a leaf to outside. This term is sometimes referred to as leaf resistance to distinguish it from the resistance due to the stomata alone. Water vapor inside leaves is maintained at or very near its saturated value, for otherwise the mesophyllic cells of the leaf would desiccate and the leaf wilt. The stomata are pores which, when open, are the main conduits for transpired water. Hence, the net resistance r_s to water passing from the inside to the outside of the leaf depends largely on the size, distribution, and degree of opening of these stomata. However, some water diffusion also occurs through leaf cuticles, which can be the primary route for transpiration when the stomata are closed. In general, the opening of the stomata, and hence r_s, changes with various environmental parameters, including inability of roots to supply adequately the transpiration demand.

The stomatal resistance factor is taken to be

$$r_s = r_{smin} \times R_f \times S_f \times M_f \times V_f. \tag{59}$$

The factors on the right–hand side are discussed, e.g., by Jarvis (1976), Hinckley *et al.* (1978); R_f gives the dependence of r_s on solar radiation. Studies have been made of the dependence of r_s on visible fluxes (cf. e.g., Hinckley *et al.*, 1978, Figure 3; Watts, 1977, Figures 10–11; Denmead and Millar, 1976, Figure 1). These studies show that a minimum stomatal resistance is reached from between 10% of full sun (approximately true for the trees studied) and full sun as indicated by Denmead for wheat. Full sun corresponds to about 500 W m^{-2} of incident visible solar radiation ($\lambda < 0.7\mu$m). The factor R_f varies between about 1 for overhead sun and r_{smax}/r_{smin} for nighttime, where r_{smax} is the cuticular resistance of the leaves. It is assumed to be of the form

$$R_f = \frac{1+f}{f + r_{smin}/r_{smax}}, \tag{60a}$$

where $f = F_v/F_{vc}$ with $r_{smax} = 5000$ s m^{-1}, F_v = flux of visible solar radiation, and F_{vc} the visible solar flux for which R_f is about double its minimum value. Present model values are $F_{vc} = 30$ W m^{-2} for trees, and $F_{vc} = 100$ W m^{-2} for grasslands and crops. The dependence of stomatal resistance on vapor pressure deficit is given by

$$V_f = 1/max(0.1, 1 - 0.025 v_{pd}) \tag{60b}$$

where v_{pd} is the departure from saturation vapor pressure inside the leaf boundary layer and evaluated by

$$v_{pd} = (1 - r'')(q_s - q_{af})(1000/0.622) \tag{60c}$$

The inverse of equation (60a) is averaged over a number of layers in the canopy ($I_{max} = 4$) which receive different amounts of radiation and over streams of direct

and diffuse solar radiation, neglecting scattering within the canopy (since the different layers contribute in parallel to resistance, it is conductance that is averaged). Thus

$$1/R_f = \sum_{i=1}^{I_{max}} \frac{f_i + r_{smin}/r_{smax}}{1 + f_i} / I_{max} \tag{60d}$$

where f_i is the sum of incident contributions to f from direct and diffuse radiation in a layer,

$$f_i = f_{iI} + f_{iD} \tag{60e}$$

For the top canopy layers,

$$f_{iI} = (1 - T_L) F_{vi} / F_{vc} \; I_{max} / L_{SAI} \tag{60f}$$

$$f_{iD} = (1 - T_{LD}) F_{viD} / F_{vc} \; I_{max} / L_{SAI} \tag{60g}$$

where F_{vi} is the direct beam incident visible and F_{viD} is the corresponding diffuse radiation, T_L is the canopy layer transmittance to the direct beam, neglecting stems, i.e.,

$$T_L = exp[-G^L L_{SAI} / \mu I_{max}] \tag{60h}$$

where G^L is the average leaf projection factor (we take $G^L = 0.5$) and μ = cosine of solar zenith. The diffuse beam transmittance T_{LD} is the same as Eq. (60h) with $\mu = 0.5$. Below the top layer

$$f_{iI} = f_{i-1,I} T_L \tag{60i}$$

$$f_{iD} = f_{i-1,D} T_{LD} \tag{60j}$$

The seasonal temperature factor $S_f = 1/F_{SEAS}(T_f)$, is given by Eq. (1c). The moisture factor M_f depends on the soil moisture and the ability of plant roots to

take water readily from the soil for a given level of root moisture. Initially, M_f = 1, and if the plants' transpiration exceeds a maximum value, depending on soil moisture as described below, M_f is increased so that the transpiration is maintained at the maximum value. Finally, if r_s as given by Eq. (59) exceeds r_{smax}, it is set to r_{smax}.

e. Root Resistance

The transpiration rate calculated from Eq. (58) must be consistent with the maximum transpiration that the vegetation can sustain as defined below. If E_{tr} is found to exceed E_{trmx}, then r_s is redetermined so that $E_{tr} = E_{trmx}$, the maximum transpiration available from the plant. The determination of this maximum is based on a simplification of the SPAC (Soil Plant Atmosphere Continuum) model of Federer (1979). For reviews of root–water models, see Hillel (1980) and Molz (1981). The plant water uptake in each soil layer is limited by the difference between soil and the leaf potential divided by an effective resistance. This effective resistance depends on the total length of root per unit area and the internal plant resistance per unit root length. When the soil is dry enough, the diffusion of water from the soil to the roots also contributes to this resistance. Lumping various terms together yields the following formula,

$$E_{trmx} = \Upsilon_{r0} \, \Sigma_i \, R_{ti} \, (1 - W_{LT}^i), \tag{61}$$

where Υ_{r0} is the maximum transpiration that can be sustained. The sum is over soil layers, each designated by subscript i, R_{ti} is the fraction of roots in a given soil layer, and W_{LT}^i is a soil dryness (or plant wilting) factor. We have taken $\Upsilon_{r0} = 2 \times 10^{-4}$ mm s$^{-1} \times \sigma_f \times S_{EASB}$, where S_{EASB} is a factor that is 1 during the growing season and drops to 0 when the soil is frozen. For typical vegetation, $\sigma_f = 0.8$, and close to field capacity, $W_{LT}^i = 0.05$ so that typically for well–watered growing season vegetation, $\Upsilon_{r0} = 1.5 \times 10^{-4}$ mm s^{-1}, corresponding to a maximum latent energy flux of about 380 W m^{-2}. Observed latent fluxes from unwetted foliage under intense solar radiation rarely exceed 400 W m^{-2}. Federer (1979, cf. his Figure

1), modeling data for birch and maple forests, finds maximum transpiration of about 1.5×10^{-4}mm s^{-1}, although with sufficient root capacity the transpiration could exceed 2.0×10^{-4}mm s^{-1}.

The negative of the leaf potential can be approximated by the maximum value it takes before leaf desiccation, since the leaf potentials of many plants approach this value under any significant water stress. The term W_{LT}^i then is $(\phi - \phi_0)$ divided by $(\phi_{max} - \phi_0)$, where ϕ is the soil water suction and ϕ_{max} is the maximum value of negative of potential of leaves before desiccation. Hence, for soil suction of the form given in section 4c,

$$W_{LT}^i = \frac{s_i^{-B} - 1}{s_w^{-B} - 1}, \tag{62}$$

where s_i is the soil water of the i'th layer and s_w the soil water for which transpiration essentially goes to zero, defined here as the soil water at which suction reaches 15 bars. Soils of clay–like texture would have larger values and sandy–textured soils lower values. The factor W_{LT}^i ranges from 0 at saturation to 1 at the "permanent wilting point."

The ratio of maximum water extraction, given by Eq. (61) for a given soil layer, to the maximum water extraction for the rooting zone multiplied by the fraction of roots in the given layer gives the fraction of total transpiration that is taken from the given layer. This permits a variable distribution of roots between the upper soil layer and the total active soil column. The parameter $ROOTF$ as given in Table 2 is the ratio of the density of the roots in the upper layer to the density of roots in the total column. Thus, e.g., for a 1 m total rooting zone and 20 cm upper layer, if $ROOTF = 5$, then 50% of the roots is in the upper soil layer.

f. Energy Balance of Plant Canopy and Soil

The air within the canopy has negligible heat capacity and so heat flux from the foliage H_f and from the ground H_g must be balanced by heat flux to the atmosphere H_a, i.e.,

$$H_a = H_f + H_g, \tag{63}$$

where flux to the atmosphere is given by

$$H_a = \rho_a \sigma_f C_p C_D V_a (T_{af} - T_a), \tag{64}$$

where C_p is the specific heat of air, V_a is the magnitude of atmospheric wind above the canopy, and C_D is the aerodynamic bulk transfer coefficient between canopy air and atmosphere above, assumed to be the same for heat and moisture as for momentum. The flux from the soil under the canopy is assumed to be

$$H_g = \rho_a C_p \left[C_{SOILC}\ \sigma_f\ U_{af}\right] (T_{g1} - T_{af}). \tag{65}$$

where C_{SOILC} assumed to be 0.004 is the transfer coefficient between the canopy air and underlying soil.

Equations (63)–(65) are solved for T_{af}, i.e.,

$$T_{af} = (c_A T_a + c_F T_f + c_G T_{g1})/(c_A + c_F + c_G), \tag{66}$$

where

$$c_A = \sigma_f C_D V_a, \tag{67}$$

$$c_F = \sigma_f L_{SAI} r_{\ell a}^{-1}, \tag{68}$$

$$c_G = C_{SOILC} \sigma_f U_{af} \tag{69}$$

are conductances for heat flux, to the atmosphere above the canopy, and from foliage, and the ground, respectively. Similarly, the canopy air is assumed to have zero capacity for water vapor storage so that the flux of water from the canopy air E_a balances the flux from the foliage E_f and the flux from the ground, E_g, i.e.,

$$E_a = E_f + E_g, \tag{70}$$

where E_f was defined earlier in Eq. (56), and

$$E_a = \rho_a c_A (q_{af} - q_a), \tag{71}$$

$$E_g = \rho_a c_G f_g (q_{g,s} - q_{af}), \tag{72}$$

where $q_{g,s}$ is the saturated soil water vapor concentration and f_g is a wetness factor, defined as the ratio of actual to potential ground evaporation as obtained from the soil moisture parameterization. Equations (70-72) are solved for q_{af} i.e.,

$$q_{af} = \frac{(c_A q_a + c_V q_f^{SAT} + c_G f_g q_{g,s})}{(c_A + c_V + f_g c_G)}, \tag{73}$$

where $c_V = r'' c_F$ is the average conductance of foliage to water vapor flux.

g. Leaf Temperature

The final budget equation required to obtain the transpiration from vegetation is an equation of foliage energy conservation, i.e.,

$$R_n(T_f) = LE_f(T_f) + H_f(T_f), \tag{74}$$

where R_n is the net radiation absorbed by the foliage. Equation (74) is solved for foliage temperature T_f by Newton–Raphson iteration. In the model formulation, the emissivity of the ground and foliage is assumed to be unity; the foliage is assumed to have zero heat capacity, and photosynthetic and respiratory energy transformations are neglected. The exchange of thermal infrared (longwave) radiation from canopy to ground is approximated by

$$4\sigma T_{g1}^3 (T_f - T_{g1}),$$

and net exchange from canopy to sky by

$$4\sigma(1-\sigma_f) T_{g1}^3 (T_f - T_{g1}) + F_{RLNK},$$

where F_{RLNK} as calculated in the radiation routine is $\sigma[\sigma_f T_f^4 + (1-\sigma_f) T_g^4] - F_{LW}$, the net loss of long–wave radiation from the surface. Absorbed solar radiation S_{qf} is obtained in the radiation routine from incident solar radiation and canopy albedo as obtained from subroutine ALBEDO.

The net radiation absorbed by vegetation per unit area F_{RAD} becomes

$$F_{RAD} = S_{F1} - 4\sigma\sigma_f T_{g1}^3 T_f, \tag{75}$$

where

$$S_{F1} = \sigma_f (S_{qf} - F_{RLNK} + 4\sigma T_{g1}^4). \tag{76}$$

The previously defined resistances are calculated iteratively as T_f changes. In particular, it is necessary to reevaluate the sensible heat flux to the atmosphere and the evapotranspiration E_f (cf. Eqs. (55) – (56)) through its dependence on foliage temperature, saturation specific humidity q_f^{SAT} and through q_{af} dependence on C_D (Eq. (73)).

Thus, we expand

$$H_f^{N+1} = H_f^N + \delta H (T_f^{N+1} - T_f^N), \tag{77}$$

$$E_f^{N+1} = E_f^N + \delta E (T_f^{N+1} - T_f^N), \tag{78}$$

where H_f^N is evaluated using T_f^{N+1} but C_D af the current time step, and

$$\delta H = \frac{\partial H_f^N}{\partial C_D} \frac{\partial C_D}{\partial T_f}, \tag{79}$$

$$\delta E = \frac{\delta E_f^N}{\partial q_f^{SAT}} \frac{\partial q_f^{SAT}}{\partial T_f} + \frac{\partial E_f^N}{\partial C_D} \frac{\partial C_D}{\partial T_f}. \tag{80}$$

The expression q_f^{SAT}, as all saturation specific humidity, is calculated using

$$q^{SAT} = \frac{0.622 \times p^{SAT}}{p - 0.378 p^{SAT}}, \tag{81}$$

with p^{SAT} calculated from Tetens' formula

$$p^{SAT} = 611 \exp\left\{ \frac{A(T - T_m)}{T - B} \right\}, \tag{82}$$

where

$$A = 21.874(T \leq T_m),\ 17.269\ (T > T_m),$$

and

$$B = 7.66(T \leq T_m),\ 35.86\ (T > T_m),$$

where $T_m = 273.16$.

Hence,

$$\frac{\partial q_f^{SAT}}{\partial T_f} \doteq \frac{A(T_m - B)}{(T_f - B)^2} q^{SAT}. \tag{83}$$

We calculate T_f iteratively, as

$$T_f^{N+1} = \frac{S_f + \rho_a c_p c_H (c_A T_a + c_G T_g) + L_v (T_f^N \delta E - E^N)}{4\sigma_f \sigma T_g^3 + \rho_a c_p c_H (c_A + c_G) + L_v \delta E}, \tag{84}$$

taking

$$c_H = c_F/(c_A + c_F + c_G). \tag{85}$$

The T_f's are constrained to change by no more than 1° in one iteration. Let

$$\Delta^{N+1} = T^{N+1} - T^N,$$

and

$$\widetilde{\Delta} = \text{larger of}(\Delta^{N+1}, \Delta^N).$$

The iteration is stopped after 2 or more steps, if $\widetilde{\Delta} < 0.01$ and LE_f changed by $< 0.1/\mathrm{Wm}^{-2}$ or after forty iterations have been carried out.

After completion of the T_f calculation, we obtain

$$\Delta T_{a,f} = T_a - T_{af},$$

$$\Delta q_{a,f} = q_a - q_{af},$$

for use in obtaining sensible and latent heat fluxes to the atmosphere, and update the leaf water budget by adding the difference between the foliage evapotranspiration and its water vapor flux to the atmosphere. Leaf water can either increase because of dew formation or decrease because of evaporation of leaf water.

h. Fluxes From Unvegetated Fraction

The fluxes of sensible heat and latent heat from the unvegetated fraction of soil surface F_{BARE} and Q_{BARE} are given by

$$F_{BARE} = W_G(T_{g1} - T_s) \tag{86a}$$

$$Q_{BARE} = W_G(q_g - q_s) \tag{86b}$$

$$W_G = C_D(1-\sigma_f)\{(1-\sigma_f)V_a + \sigma_f[X_B U_{af} + (1-X_B)V_a]\} \tag{87}$$

with

$$X_B = \min(1,\ R_{OUGH})$$

The term W_G is tailored to a) go to bare soil limit $(1-\sigma_f)\ C_D V_a$ as $\sigma_f \to 0$; b) go to the same limit over short vegetation but go to the limit $(1-\sigma_f)C_D U_{af}$ for tall vegetation.

A newer version of the solution coupling to the soil surface temperature calculation includes increments as in Eq. (77) and (78) to correct the $N+1$ step soil temperature as well.

7. SOIL MOISTURE WITH VEGETATION

In the presence of vegetation the soil moisture and snow cover, Eqs. (27a), (27b), (28), and (40) become

$$\frac{\partial S_{sw}}{\partial t} = P_r(1-\sigma_f) - R_s + \Upsilon_{w1} - \beta E_{tr} - F_q + S_m + D_w, \tag{86}$$

$$\frac{\partial S_{rw}}{\partial t} = P_r(1-\sigma_f) - R_s + \Upsilon_{w2} - E_{tr} + S_m + D_w \tag{87}$$

$$\frac{\partial S_{tw}}{\partial t} = P_r(1-\sigma_f) - R_w - E_{tr} - F_q + S_m + D_w, \tag{88}$$

$$\frac{\partial S_{cv}}{\partial t} = P_s(1-\sigma_f) - F_q - S_m + D_s, \tag{89}$$

where β = fraction of transpiration from the top soil layer, D_w is the rate of excess water dripping from leaves per unit land area, D_s is the corresponding rate at which excess snow falls from the leaves, as mentioned following Eq. (52), and $R_w = R_s + R_g$ is the total runoff.

APPENDIX A. Fortran Symbols for Some Parameters in Model Code

(Units are in parentheses; no units indicate a dimensionless parameter)

AGE	Factor to reduce visible snow albedo due to age of snow
AGE1	Snow aging factor due to crystal growth
AGE2	Snow aging factor due to surface melting
AGE3	Snow aging factor due to accumulation of other particles
ALBGL	Albedo, soil, near–infrared, direct
ALBGLD	Albedo, soil, near–infrared, diffuse
ALBGS	Albedo, soil, visible, direct
ALBGSD	Albedo, soil, visible, diffuse
ALBL	Albedo, vegetation, near–infrared, direct
ALBLD	Albedo, vegetation, near–infrared, diffuse
ALBS	Albedo, vegetation, visible, direct
ALBSD	Albedo, vegetation, visible, diffuse
ALBZN	Zenith angle correction for albedo
BSW	Soil diffusivity parameter (= B in Clapp & Hornberger, 1978)
CDR	Surface drag coefficient
CDRN	Surface drag coefficient for neutral stability
CDRX	Surface drag coefficient for ice with leads
CF	Heat transfer coefficient from leaves
CH20	Specific heat of water (J m^{-3} K^{-1})
CICE	Specific heat of ice (J m^{-3} K^{-1})
CLND	Proportionality factor (to the ocean) for drag coefficient over land
COSZRS	Cosine of solar zenith angle (radians)
CROUGH	Proportionality factor (to the ocean) for drag coefficient over vegetation
CZF	Correction term for new snow albedo for large solar zenith angle
DENSI	Ratio of snow density to fresh snow density

DEPA	Depth of active soil column (mm)
DEPU	Depth of top soil layer (mm)
DEWMX	Maximum allowed depth of water on leaves (mm)
DMAX	Maximum soil diffusivity (m^2 s^{-1})
DRAIN	Hydraulic conductivity at bottom of total (10 m) soil layer.
DTLAF	Difference between leaf temperature and temperature of air in foliage
EF	Moisture flux from foliage (mm s^{-1})
EFPOT	Potential evaporation rate from foliage (mm s^{-1})
EFPR	Maximum evapotranspiration sustainable by the leaves, given the soil moisture (mm s^{-1}
EMS	Atmospheric emissivity
ETR	Transpiration rate (mm s^{-1})
ETRC	Maximum possible transpiration, given the soil moisture (mm s^{-1})
EVMX0	Maximum evaporation at saturation (mm s^{-1})
FACT	Turbulent removal flux coefficient
FB	Fractional intercepted visible radiation absorbed in lower canopy
FC	Light sensitivity factor for crops and grasses (m^2 W^{-1})
FDRY	Fraction of foliage that is green and dry
FEVPG	Evaporative heat flux from ground (mm s^{-1})
FLMX	Maximum rate of infiltration allowed by soil (mm s^{-1})
FSEAS	Function for temperature dependence of, vegetation cover
FSENG	Sensible heat flux from ground (W m^{-2})
FT	Fractional intercepted visible radiation absorbed in upper canopy
FWET	Fraction of foliage covered by water
GWATR	Net input of water to the soil surface (mm)
GWMX	Maximum soil moisture content (mm)
HS	Net energy flux into the surface (W m^{-2})
HSF	Sensible heat from leaves (W m^{-2})

HTVP	Latent heat of vaporization of water (or sublimation) (J kg^{-1})
LVEG	Vegetation type
PHI0	Minimum soil suction (mm)
PORSL	Soil porosity ratio
QSAT	Saturated specific humidity (kg kg^{-1})
RA	Aerodynamic resistance factor for leaves
RAP	Potential rate of evaporation (mm s^{-1})
RHOSW	Density of snow relative to water
RIB	Surface bulk Richardson number
RLAI	Inverse of sum of leaf area index and stem area index
RMAX0	Maximum stomatal resistance (s m^{-1})
RNOF	Summed runoff (= RSUR + RSUBS) (mm s^{-1}) Surface and total runoff terms are accumulated at the end of subroutine WATER so that output values are in mm day^{-1}
ROTF	Ratio of soil moisture extraction from top to total, when fully saturated
ROUGH	Aerodynamic roughness length (m)
ROUGHG	Proportionality factor (to the ocean) for drag coefficient over total surface
RS	Stomatal resistance (s m^{-1})
RSCS	Heat capacity of soil (J kg^{-1})
RSMIN	Minimum stomatal resistance (s m^{-1})
RSUBS	Subsurface drainage (mm s^{-1})*
RSUR	Surface runoff (mm s^{-1})*
SABVEG	Radiation absorbed by vegetation (W m^{-2})
SAI	Stem area index

SCOND	Term proportional to leaf transpiration water loss
SCOR	Snow surface drag coefficient correction factor
SDROP	Snow falling off vegetation
SEASB	Seasonal factor depending on lower soil temperature and controlling LAI and root water uptake
SEASF	Difference between VEGC and fractional cover at 269 K
SG	Solar flux absorbed by bare ground (W m^{-2})
SIGF	Fractional vegetation cover
SK	Soil heat conductivity (J m^{-1})
SM	Rate of snowmelt
SNAL0	New snow albedo, visible
SNAL1	New snow albedo, near–infrared
SOLIS	Incident visible radiation, used for stomatal resistance (W m^{-2})
SQF	Solar flux absorbed by leaf (W m^{-2})
SWILT	Soil moisture content at which permanent wilting occurs (mm)
SWTRT	Average soil moisture per unit volume of soil, weighted toward top
TAF	Temperature of air in canopy (K)
TAU1	Length of day (s)
TG	Temperature of soil at surface (K)
TGB	Temperature of subsoil
TM	A reference temperature = TS − 2.2 (K)
TRANS0	Movement of water from below to upper soil layer (mm s^{-1})
TRANS1	Net drying out of upper layer (mm s^{-1})
TRSMX	Maximum transpiration rate at saturation allowing for fractional vegetation cover and seasonal temperature dependence (mm s^{-1})
TRSMX0	Maximum rate of transpiration with saturated soil, 100% vegetation, optimum temperature (mm s^{-1})
TS	Temperature of air above canopy (K)

TVEG	Vegetation type
UAF	Velocity of air within foliage (m s^{-1})
VA	Wind speed above canopy (m s^{-1})
VEGC	Maximum fractional cover of vegetation
WATA	Average of WATR and WATU
WATR	Ratio of root zone soil moisture to maximum allowance.
WATT	Ratio of total soil moisture to maximum allowed
WATU	Ratio of upper soil moisture to maximum allowed
WILTR	Fractional soil moisture at which permanent wilting occurs
WLTTB	Wilting factor for root zone
WLTUB	Wilting factor for upper soil
WT	Fraction of grid square covered by snow
XKMX	Maximum soil hydraulic conductivity (mm s^{-1})
XLA	Maximum leaf area index
XLAI	Leaf area index
XLAI0	Minimum leaf area index
XRUN	Leaf drip (mm s^{-1})
ZLND	z_o for bare soil
ZOCE	z_o for water
ZSNO	z_o for snow

APPENDIX B. Pointers Defining Location of Boundary Subroutine Variables*

NPK	Surface pressure
NDRAGK	Drag or surface stress
NDELTK	Temperature difference between above–canopy air and foliage air
NDELQK	Specific humidity difference between above–canopy air and foliage air
NZBK	Surface elevation
NTGK	Temperature of the soil surface
NTSK	Temperature of the air above canopy
NQGK	Specific humidity at soil surface
NQSK	Specific humidity above canopy
NUSK	Westerly wind above canopy
NVSK	Southerly wind above canopy
NLDOCK	Land/ocean mask (0 = ocean, 1 = land, 2 = sea ice)
NSWTK	Not used
NSCVK	Snow cover, water equivalent
NRNOK	Total runoff
NRNOSK	Surface runoff
NTGBK	Temperature of lower soil layer
NSICEK	Thickness of sea ice
NSAGK	Snow age, nondimensional
NLDEWK	Depth of water on foliage
NTLEFK	Temperature of foliage
NEVPAK	Moisture flux, averaged over history–write interval
NSENAK	Sensible heat flux, averaged over history–write interval
NTGAK	Soil surface temperature, averaged over history–write interval
NTSAK	Above–canopy air temperature, averaged over history–write interval
NPRCAK	Precipitation, averaged over history–write interval
NFRLAK	Net infrared energy flux, averaged over history–write interval
NFRSAK	Net absorbed solar energy flux, averaged over history–write interval
NGWETK	Soil wetness factor, i.e., ratio of evaporation to that from a wet soil
NTMINK	Minimum above–canopy temperature, over history–write interval
NTMAXK	Maximum above–canopy temperature, over history–write interval
NVEGK	Fractional vegetation cover
NEVPRK	Moisture flux to atmosphere
NSENTK	Sensible heat flux to atmosphere
NZ1K	Altitude of lowest atmospheric level
NRHSK	Density of surface air
NSSWK	Water in upper soil
NPBPK	Accumulated carbon uptake
NRFEK	Number of rainfall events
NLREK	Accumulated duration of rainfall events
NQSAK	Specific humidity above canopy, averaged over history–write interval

NRESPK	Accumulated carbon uptake of soil and vegetation minus carbon loss by respiration
NPRCPK	Instantaneous precipitation rate
NIRCPK	Intercepted precipitation rate
NPRDK	Currently not used
NTAFK	Temperature of the air within foliage
NSFK	Solar energy flux
NGWETK	Soil wetness factor - ratio of evaporation to potential rate
NRSWK	Root zone water
NTWSK	Total soil water
NFRLK	Net infrared energy flux at surface
NFRSK	Net absorbed solar energy flux
NTVEGK	Vegetation type (see Table 1)

*Listed in order of occurrence in the common block BPNT.

REFERENCES

Anderson, E. A., 1976: *A Point Energy and Mass Balance Model of a Snow Cover.* Office of Hydrology, National Weather Service, 150 pp.

Barry, R. G. and R. E. Chambers, 1966: A preliminary map of summer albedo over England and Wales. *Quart. J. Roy. Meteor. Soc.,* **92,** 543–548.

Campbell, G. S., 1974: A simple method for determining unsaturated conductivity from moisture retention data. *Soil Science,* **117,** 311–314.

Clapp, R. B. and G. M. Hornberger, 1978: Empirical equations for some soil hydraulic properties. *Water Resources Research,* **14,** 601–604.

Condit, H. R., 1970: The spectral reflectance of American soils. *Photogrammetric Engineering,* **36,** 955–966.

Deardorff, J., 1978: Efficient prediction of ground temperature and moisture with inclusion of a layer of vegetation. *J. Geophys. Res.,* **83,** 1889–1903.

Denmead, O. T. and B. D. Millar, 1976: Field studies of the conductance of wheat leaves and transpiration. *Agron. J.,* **68,** 307–311.

de Vries, D. A., 1963: Thermal properties of soils. In *Physics of Plant Environment.* North Holland Publishing Co., 594 pp.

Dickinson, R. E., 1984: Modeling evapotranspiration for three–dimensional global climate models. In *Climate Processes and Climate Sensitivity.* J. E. Hansen and T. Takahashi, eds., American Geophysical Union, Washington, DC, 58–72.

Dickinson, R. E., J. Jaeger, W. M. Washington, and R. Wolski, 1981: *Boundary Subroutine for the NCAR Global Climate Model.* NCAR Technical Note/TN–173+1A, National Center for Atmospheric Research, Boulder, CO, 75 pp.

Dickinson, R.E., A. Henderson-Sellers, P.J. Kennedy, and M.F. Wilson, 1986: *Biosphere-Atmosphere Transfer Scheme (BATS) for the NCAR Community Climate Model*, National Center for Atmospheric Research, Boulder, CO, Tech. Note TN-275+STR.

Dickinson, R.E., 1988: The force-restore model for surface temperatures and its generalizations. *J. Climate*, **1**, No. 11, 1086-1097.

Dickinson, R. E., 1991: Global change and terrestrial hydrology: A review, *Tellus*, **43AB**, 176-181.

Dickinson, R. E. and P. J. Kennedy, 1991: Land surface hydrology in a general circulation model: Global and regional fields needed for validation, *Surv. in Geophys.* **12**, 115-126.

Dickinson, R.E. and P.J. Kennedy, 1992: Impacts on regional climate of amazon deforestation, *Geophys. Res. Letters*, **19**, 1947-1950.

Dickinson, R. E., R. M. Errico, F. Giorgi, and G. T. Bates, 1989: A reginal climate model for the western United States, *Climatic Change*, **15**, 383-42.

Dickinson, R. E., A. Henderson-Sellers, C. Rosenzweig, and P. J. Sellers, 1991: Evapotranspiration models with canopy resistance for use in climate models, a review, *Ag. & Forest Meteor. Journal*, **54**, 375-388.

FAO/UNESCO, 1974: *Soil Map of the World.* FAO, Paris, France.

Federer, C. A., 1968: Spatial variation of net radiation, albedo, and surface temperature of forests. *J. Appl. Meteor.,* **7,** 789–795.

Federer, C. A., 1971: Solar radiation absorbed by leafless hardwood forests. *Agricultural Meteorol.,* **9,** 1971/1972, 3–20.

Federer, C. A., 1979: A soil–plant atmosphere model for transpiration and availability of soil water. *Water Resources Research,* **15,** 555–562.

Fleming, G., 1975: *Computer Simulation Techniques in Hydrology.* Elsevier, New York, NY, 333 pp.

Fuller, S. P. and W. R. Rouse, 1979: Spectral reflectance changes accompanying a post–fire recovery sequence in a subarctic spruce lichen woodland. *Remote Sensing of Environment,* **8,** 11–23.

Garratt, J. R., 1977: Review of drag coefficients over oceans and continents. *Mon. Wea. Rev.,* **105,** 915–929.

Gates, D. M., 1980: *Biophysical Ecology.* Springer–Verlag, New York, NY, 611 pp.

Gates, D. M., M. J. Keegan, J. C. Schleter, and V. R. Weidner, 1965: Spectral properties of plants. *Appl. Optics,* **4,** 11–20.

Hillel, D., 1980: *Applications of Soil Physics.* Academic Press, New York, NY, 385 pp.

Hinckley, T. M., J. P. Lassoie, and S. W. Running, 1978: Temporal and spatial variations in the water status for forest trees. *Forest Science Monograph,* **20,** Society of American Foresters, 72 pp.

Idso, S. B., R. D. Jackson, R. J. Reginato, B. A. Kimball, and F. S. Nakayama, 1975: The dependence of bare soil albedo on soil water content. *J. Appl. Meteor.,* **14,** 109–113.

Jarvis, P. G., 1976. The interpretation of the variations in leaf water potential and stomatal conductance found in canopies in the field. *Philos. Trans. Roy. Soc. London*, **Ser. B, 273**, 593-610.

Kirby, M. J., Ed., 1979: *Hillslope Hydrology.* Wiley, New York, NY, 338 pp.

Kondratyev, K. Ya., 1969: *Radiation in the Atmosphere.* Academic Press, New York, NY, 912 pp.

Kriebel, K. T., 1979: Albedo of vegetated surfaces: Its variability with differing irradiances. *Remote Sensing of the Environment,* **8,** 283–290.

Kukla, G. J. and D. Robinson, 1980: Annual cycle of surface albedo. *Mon. Wea. Rev.,* **108,** 56–67.

Kung, E. C., R. A. Bryson, and D. H. Lenschow, 1964: Study of a continental surface albedo on the basis of flight measurements and structure of the earth's surface cover over North America. *Mon. Wea. Rev.,* **92,** 543–564.

L'vovich, M. I., 1979: *World Water Resources and Their Future.* American Geophysical Union, Washington, DC, 415 pp.

Marshall, S.E., 1989: A physical parameterization of snow albedo for use in climate models. Ph.D. thesis, U. Washington, 161 pp.

Massman, W. J., 1980: Water storage on forest foliage: A general model. *Water Resources Research,* **16,** 210–216.

Matthews, E., 1983: Global vegetation and land use: New high resolution data bases for climate studies. *J. Clim. Appl. Meteor.,* **22,** 474–487.

Matthews, E., 1984: Prescription of land–surface boundary conditions in GISS GCMII and Vegetation, land–use and seasonal albedo data sets: Documentation of archived data tape. *NASA Technical Memos 86096 and 86107,* NASA, Goddard Institute for Space Studies, New York, NY, 20 pp. and 9 pp.

Maykut, G. and N. Untersteiner, 1971: Some results from a time–dependent thermodynamic model of sea ice. *J. Geophys. Res.,* **76,** 1550–1575.

Mearns, L.O., S.H. Schneider, S.L. Thompson and L.R. McDaniel, 1990: Analysis of climate variability in general circulation models: Comparison with observations and changes in variability in 2xCO_2 experiments, *J. Geophs. Res.* **95(12)**, 20469-20490.

Molz, F. J., 1981: Models of water transport in the soil–plant system: A review. *Water Resources Research,* **17,** 1245–1260.

Monteith, J. L., 1959: The reflection of short–wave radiation by vegetation. *Quart. J. Roy. Meteor. Soc.,* **85,** 386–392.

Oguntoyinbo, J. S., 1970: Reflection coefficient of natural vegetation, crops and urban surfaces in Nigeria. *Quart. J. Roy. Meteor. Soc.* **96,** 430–441.

Olson, J. S., J. A. Watts, and L. J. Allison, 1983: Carbon in live vegetation of major world ecosystems. U.S. Department of Energy, DOE/NBB–0037, No. TR004, U.S. Department of Energy, Washington, DC, 152 pp.

Pitman, A. J., A. Henderson-Sellers, and Z. L. Yang, 1990: Sensitivity of regional climates to localized precipitation in global models, *Nature*, **346**, 734-737.

Ripley, E. A. and R. E. Redman, 1976: Grassland. In Monteith, *loc. cit.,* p. 351.

Rockwood, A. A. and S. K. Cox, 1978: Satellite inferred surface albedo over northwestern Africa. *J. Atmos. Sci.,* **35,** 513–522.

Semtner, A. J., 1976: A model for the thermodynamic growth of sea ice in numerical investigations of climate. *J. Phys. Oceanogr.,* **6,** 379–389.

Shuttleworth, W. J., 1978: A simplified one–dimensional theoretical description of the vegetation–atmosphere interaction. *Boundary–Layer Meteor.,* **14,** 3–27.

Stewart, J. B., 1971: The albedo of a pine forest. *Quart. J. Roy. Meteor. Soc.,* **97,** 561–564.

Thom, A. S. and H. R. Oliver, 1977: On Penman's equation for estimating regional evaporation. *Quart. J. Roy. Meteor. Soc.,* **103,** 345–357.

Tucker, C. J. and L. D. Miller, 1977: Soil spectra contributions to grass canopy spectral reflectance. *Photogrammatic Engineering and Remote Sensing,* **43,** 721–726.

U.S. Corps of Engineers, 1956: *Snow Hydrology,* 437 pp.

Watts, W. R., 1977: Field studies of stomatal conductance. In *Environmental Effects in Crop Physiology.* J. J. Landsberg and C. V. Cutting, eds., Academic Press, New York, NY, 388 pp.

Wilson, M. F., 1984: The construction and use of land surface information in a general circulation climate model. Unpublished Ph.D. thesis, University of Liverpool, United Kingdom, 346 pp.

Wiscombe, W. J. and S. G. Warren, 1980: A model for the spectral albedo of snow. I. Pure snow, *J. Atmos. Sci.*, **37**, 2712-2733.

Yen, Y.-C., 1969: Recent studies in snow properties. In *Advances in Hydrosciences*, **5**, Academic Press, New York, NY, 305 pp.

BATS Publications

Bonan, G.B., 1994: Comparison of the land surface climatology of the National Center for Atmospheric Research community climate model 2 at R15 and T42 resolutions. *J. Geophys. Res.*, **99**, 10,357-10,364.

Crosson, W.L., H.J. Cooper, and E.A. Smith, 1993: Estimation of surface heat and moisture fluxes over a prairie grassland. Part 4: Impact of satellite remote sensing of slow canopy variables on accuracy of a hybrid biosphere model. *J. Geophys. Res.*, **98**, 4979-4999.

Dickinson, R.E., 1984: Modelling evapotranspiration for three-dimensional global climate models. *Climate Processes and Climate Sensitivity*, Geophysical Monograph 29, Maurice Ewing Volume 5, J.E. Hansen and T. Takahashi, Eds., American Geophysical Union, Washington, D.C., 58-72.

Dickinson, R.E., 1987: Evapotranspiration in global climate models. *Adv. Space Res.*, **7**, (11)17-(11)26.

Dickinson, R.E., 1988: The force-restore model for surface temperatures and its generalizations. *J. Climate*, **1**, 1086-1097.

Dickinson, R.E., 1989a: Implication of tropical deforestation for climate: a comparison of model and observational descriptions of surface energy and hydrological balance. *Phil. Trans. Roy. Soc. London*, **B234**, 423-431.

Dickinson, R.E., 1989b: Modelling the effects of Amazonian deforestation on regional climate: a review. *Argic. For. Meteorol.*, **47**, 339-347.

Dickinson, R.E., 1990: Water and energy exchange. *Remote Sensing of Biosphere Functioning*, R.J. Hobbs and H.A. Mooney, Eds., Springer-Verlag New York, Inc., 105-133.

Dickinson, R.E. and A. Henderson-Sellers, 1988: Modelling tropical deforestation: A study of GCM land-surface parameterizations. *Quart. J. Roy. Meteor. Soc.*, **114**, 439-462.

Dickinson, R.E. and P.J. Kennedy, 1991: Land surface hydrology in a general circulation model-global and regional fields needed for validation. *Surveys in Geophysics*, **12**, 115-126.

Dickinson, R.E., A. Henderson-Sellers, and P.J. Kennedy, 1993: Biosphere Atmosphere Transfer Scheme (BATS) Version 1e as Coupled to the NCAR Community Climate Model. NCAR Technical Note, NCAR, 72 pp.

Dickinson, R.E., R.M. Errico, F. Giorgi, and G.T. Bates, 1989: A regional climate model for the western United States. *Clim. Change*, **15**, 383-422.

Dickinson, R.E., A. Henderson-Sellers, P.J. Kennedy, and M.F. Wilson, 1986: Biosphere Atmosphere Transfer Scheme (BATS) for the NCAR Community Climate Model. NCAR Technical Note, NCAR, TN275+STR, 69 pp.

Dickinson, R.E., A. Henderson-Sellers, C. Rosenzweig, and P.J. Sellers, 1991: Evapotranspiration models with canopy resistance for use in climate models, a review. *Agric. For. Meteor.*, 373-388.

Dickinson, R.E., J. Jager, W.M. Washington, and R. Wolski, 1981: Boundary subroutine for the NCAR global climate model. NCAR Technical Note, NCAR/TN-173+IA, June 1981, 75 pp.

Ducoudre, N.I., K. Laval, and A. Perrier, 1993: SECHIBA, a new set of parameterizations of the hydrologic exchange at the land-atmospheric interface within the LMD atmospheric general circulation model. *J. Climate*, **6**, 248-273.

Garratt, J.R., P.B. Krummel, and E.A. Kowalczyk, 1993: The surface energy balance at local and regional scales-A comparison of general circulation model results with observations. *J. Climate*, **6**, 1090-1109.

Giorgi, F., 1990a: Simulation of regional climate using a limited area model nested in a general circulation model. *J. Climate*, **3**, 941-963.

Giorgi, F., 1990b: Sensitivity of wintertime precipitation and soil hydrology simulation over the western United States to lower boundary specifications. *Atmosphere-Ocean*, **28**, 1-23.

Giorgi, F. and G.T. Bates, 1989: The climatological skill of a regional model over complex terrain. *Mon. Wea. Rev.*, **117**, 2325-2347.

Giorgi, F. and L.O. Mearns, 1991: Approaches to the simulation of regional climate change: A review. *Rev. Geophys.*, **29**, 191-216.

Giorgi, F., M.R. Marinucci, and G. Visconti, 1990: Use of a limited-area model nested in a general circulation model for regional climate simulation over Europe. *J. Geophys. Res.*, **95**, 18413-18431.

Giorgi, F., M.R. Marinucci, and G. Visconti, 1992: A 2XCO2 climate change scenario over Europe generated using a limited area model nested in a general circulation model. II: Climate change scenario. *J. Geophys. Res.*, **97**, 10 011-10 028.

Giorgi, F., G.T. Bates, and S.J. Nieman, 1993a: The multi-year surface climatology of a regional atmospheric model over the western United States. *J. Climate*, **6**, 75-95.

Giorgi, F., M.R. Marinucci, and G.T. Bates, 1993b: Development of a second generation regional climate model (RegCM2). Part I: Boundary-layer and radiative transfer processes. *Mon. Wea. Rev.*, **121**, 2794-2813.

Giorgi, F., M.R. Marinucci, G.T. Bates, and G. De Canio, 1993c: Development of a second generation regional climate model (RegCM2). Part II: Convective processes and assimilation of lateral boundary conditions. *Mon. Wea. Rev.*, **121**, 2814-2832.

Giorgi, F., S.W. Hostetler, and C.S. Brodeur, 1994a: Analysis of the surface hydrology in a regional climate model. *Quart. J. Roy. Meteor. Soc.*, **120**, 161-183.

Giorgi, F., C.S. Brodeur, and G.T. Bates, 1994b: Regional climate change scenarios over the United States produced with a nested regional climate model. *J. Climate*, **7**, 375-399.

Hahmann, A.N., D.M. Ward, and R.E. Dickinson, 1994: Surface land temperature and radiative fluxes response of the NCAR CCM2/BATS land surface scheme to modifications in the optical properties of clouds. *J. Geophys. Res.*, (submitted).

Henderson-Sellers, A. and K. McGuffie, 1987: *A Climate Modelling Primer.* John Wiley & Sons, New York/Toronto/Brisbane, 217pp.

Henderson-Sellers, A., 1990: Predicting generalized ecosystem groups with the NCAR CCM: first steps towards an interactive biosphere. *J. Climate*, **3**, 917-940.

Henderson-Sellers, A., A.J. Pitman, and R.E. Dickinson, 1990: Sensitivity of the surface hydrology to the complexity of the land-surface parameterization scheme employed. *Atmosfera*, **3**, 183-201.

Henderson-Sellers, A. and A.J. Pitman, 1992: Land-surface schemes for future climate models: Specification, aggregation, and heterogeneity. *J. Geophys. Res.*, **97**, 2687-2696.

Henderson-Sellers, A., 1993: A factorial assessment of the sensitivity of the BATS land-surface parameterization scheme. *J. Climate*, **6**, 227-247.

Henderson-Sellers, A., Z.-L. Yang, and R.E. Dickinson, 1993a: The Project for Intercomparison of Land-surface Parameterization Schemes. *Bull. Amer. Meteor. Soc.*, **74**, 1335-1349.

Henderson-Sellers, A., R.E. Dickinson, T.B. Durbidge, P.J. Kennedy, K. McGuffie, and A.J. Pitman, 1993b: Tropical deforestation: Model local- to regional-scale climate change. *J. Geophys. Res.*, **98**, 7289-7315.

Henderson-Sellers, A., J. Polcher, P.K. Love, K. MuGuffie, T.H. Chen, P. Irannejad, A.J. Pitman, Z.-L. Yang, Y. Shao, and A. Robock, 1994: How well do current landsurface models simulate the continental climate?. *Clim. Dynamics*, (submitted).

Horel, J.D., J.B. Pechmann, A.N. Hahmann, and J.E. Geisler, 1994: Simulations of the amazon basin circulation with a regional model. *J. Climate*, **7**, 56-71.

Lakhtakia, M.N. and T.T. Warner, 1994: A comparison of simple and complex treatments of surface hydrology and thermodynamics suitable for mesoscale atmospheric models. *Mon. Wea. Rev.*, **122**, 880-896.

Marinucci, M.R. and F. Giorgi, 1992: A 2XCO2 climate change scenario over Europe generated using a limited area model nested in a general circulation model. I: Present day simulation. *J. Geophys. Res.*, **97**, 9989-10 009.

Meehl, G.A., 1994: Influence of the land surface in the Asian summer monsoon: External conditions versus internal feedbacks. *J. Climate*, **7**, 1033-1049.

Pitman, A.J., 1994: Assessing the sensitivity of a land-surface scheme to the parameter values using a single column model. *J. Climate*, **7**, 1856-1869.

Pitman, A.J., A. Henderson-Sellers, and Z.-L. Yang, 1990: Sensitivity of regional climates to localised precipitation in global models. *Nature*, **346**, 734-737.

Pitman, A.J., Z.-L. Yang, and A. Henderson-Sellers, 1993a: Sub-grid scale precipitation in AGCMS: Re-assessing the land surface sensitivity using a single column model. *Clim. Dynamics*, **9**, 33-41.

Pitman, A.J., A. Henderson-Sellers, F. Abramopoulos, R. Avissar, G. Bonan, A. Boone,, R.E. Dickinson, M. Ek, D. Entekhabi, J. Famiglietti,, J.R. Garratt, M. Frech, A. Hahmann, R. Koster, E. Kowalczyk, K. Laval, J. Lean, T.J. Lee, D. Lettenmaier, X. Liang, J.-F. Mahfouf, L. Mahrt, P.C.D. Milly, K. Mitchell, N. de Noblet, J. Noilhan, H. Pan, R. Pielke, A. Robock, C. Rosenzweig, C.A. Schlosser, R. Scott, M. Suarez, S. Thompson, D. Verseghy, P. Wetzel, E. Wood, Y. Xue, Z.-L. Yang, and L. Zhang, 1993b: Project for Intercomparisons of Land-surface Parameterization Schemes (PILPS): Results from Off-line Control Simulations (Phase 1a). IGPO Publication Series, No. 7, December 1993, 47 pp.

Seth, A., F. Giorgi, and R.E. Dickinson, 1994: Simulating fluxes from heterogeneous land surfaces: Explicit subgrid method employing the biosphere-atmosphere transfer scheme (BATS). *J. Geophys. Res.*, **99**, 18,651-18,667.

Shuttleworth, W.J. and R.E. Dickinson, 1989: Comments on 'Modelling tropical deforestation: A study of GCM land-surface parameterization' by R.E. Dickinson and A. Henderson-Sellers. *Quart. J. Roy. Meteor. Soc.*, **115**, 1177-1179.

Smith, C.B., M.N. Lakhtakia, W.J. Capehart, and T.N. Carlson, 1994: Initialization of soil-water content in regional-scale atmospheric prediction models. *Bull. Amer. Meteor. Soc.*, **75**, 585-593.

Smith, E.A., W.L. Crosson, H.J. Cooper, and H.-Y. Weng, 1993: Estimation of surface heat and moisture fluxes over a prairie grassland. Part 3: Design of a hybrid physical/remote sensing biosphere model. *J. Geophys. Res.*, **98**, 4951-4978.

Ward, D.M., 1994: Comparison of the surface solar radiation budget derived from satellite data with that simulated by the NCAR CCM2. *J. Climate*, (submitted).

Washington, W.M. and C.L. Parkinson, 1986: *An introduction to three-dimensional climate modeling.* Oxford Uni. Press, 422 pp.

Wilson, M.F., A. Henderson-Sellers, R.E. Dickinson, and P.J. Kennedy, 1987a: Sensitivity of the biosphere-atmosphere transfer scheme (BATS) to the inclusion of variable soil characteristics. *J. Clim. Appl. Meteor.*, **26**, 341-362.

Wilson, M.F., A. Henderson-Sellers, R.E. Dickinson, and P.J. Kennedy, 1987b: Investigation of the sensitivity of the land-surface parameterization of the NCAR community climate model in region of tundra vegetation. *J. Climatol.*, **7**, 319-343.

Yang, Z.-L. and R.E. Dickinson, 1994a: Validating Biosphere-Atmosphere Transfer Scheme with Russian soil moisture and meteorological observational data. *J. Climate*, (to be submitted).

Yang, Z.-L., R.E. Dickinson, A. Robock, and K.Y. Vinnikov, 1994b: On validation of the snow sub-model of the Biosphere-Atmosphere Transfer Scheme with Russian snow cover and meteorological observational data. *J. Climate*, (submitted).

Yang, Z.-L., R.E. Dickinson, A. Henderson-Sellers, and A.J. Pitman, 1994c: Preliminary study of spin-up processes in land-surface models with the first stage data of PILPS Phase 1(a). *J. Geophys. Res.*, (submitted).

Zhang, T., 1994: Sensitivity properties of a biosphere model based on BATS and a statistical-dynamical climate model. *J. Climate*, **7**, 890-913.